Profiler Observations, Applications, and Analysis:
Techniques That Use Profiler/RASS Data to Characterize Meteorological Phenomena for Use in Air Quality Data Analysis and Forecasting

Clinton P. MacDonald
Timothy S. Dye
Mark R. Lilly
Sonoma Technology, Inc.
Petaluma, CA

American Meteorological Society
Short Course on the Fundamentals of Boundary Layer Wind and Temperature Profiling using Radar and Acoustic Techniques

Long Beach, CA, February 9-13, 2003

STI

Outline

- Background
- Mixing Depth
- Transport/Flow Patterns
- Meteorological Models

Background - Regional Air Quality Study Objectives

- NARSTO (North American Research Strategy for Tropospheric Ozone)
  - Understand the fundamental physical, chemical, and meteorological processes responsible for ozone accumulation on local and regional scales in North America
- Southern Oxidant Study
  - Determine the links among the chemical, biological, and meteorological processes that govern formation and accumulation of ozone and fine particulate aerosols
- California Regional Particulate Air Quality Study
  - Provide an improved understanding of emissions, PM_{10} and $PM_{2.5}$ composition, and dynamic atmospheric processes

Background - Local Air Quality Study Objectives

- Shasta County, California
  - Investigate the contribution of transported pollutants to local ozone exceedances
- Minnesota Pollution Control Agency
  - Characterize the ground-level ozone air quality of the Minneapolis/St. Paul region, including contributing factors of local emissions, meteorology, and regional transport to support air quality forecasting

Background - Common Thread

Meteorological processes that influence air quality

- Sunlight
- Horizontal dispersion
- Vertical mixing
- Transport
- Clouds and precipitation

Background - Instruments and Use

	Instruments				
Use	Surface	Sodar	RWP	RASS	Rawinsonde
Characterize Mixing		+	+++	++	+
Characterize Horizontal Dispersion	+	++	+++		+
Characterize Transport	+	+	++		+
Model Initialization	+	+	++	+	+
Model Evaluation	+	++	+++	++	+
Forecast Support	+	+	++	++	++

RWP = radar wind profiler **RASS = Radio Acoustic Sounding System**

Usefulness

+ Limited
++ Modest
+++ High

Background - Rawinsonde Winds

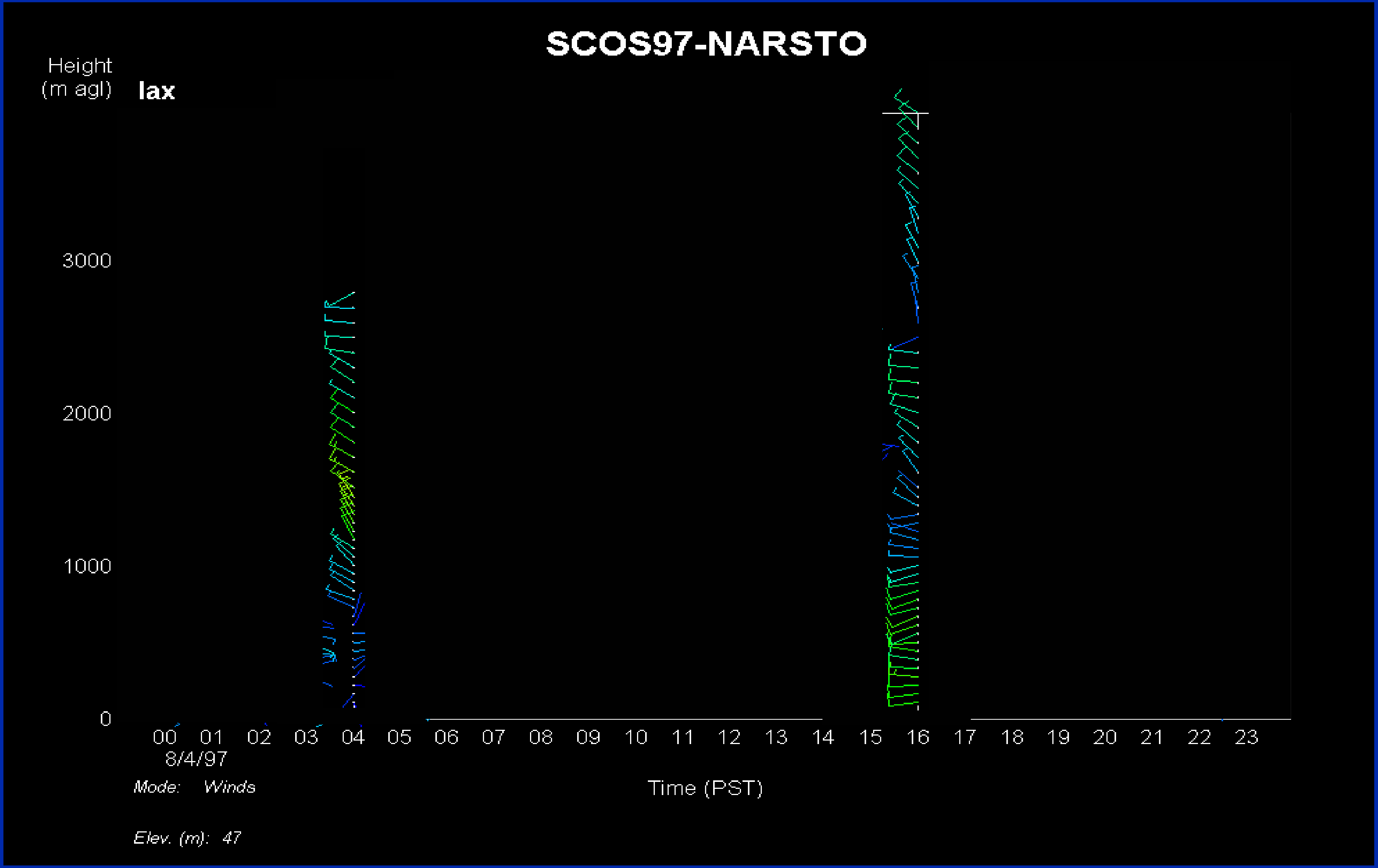

Background – RWP Winds

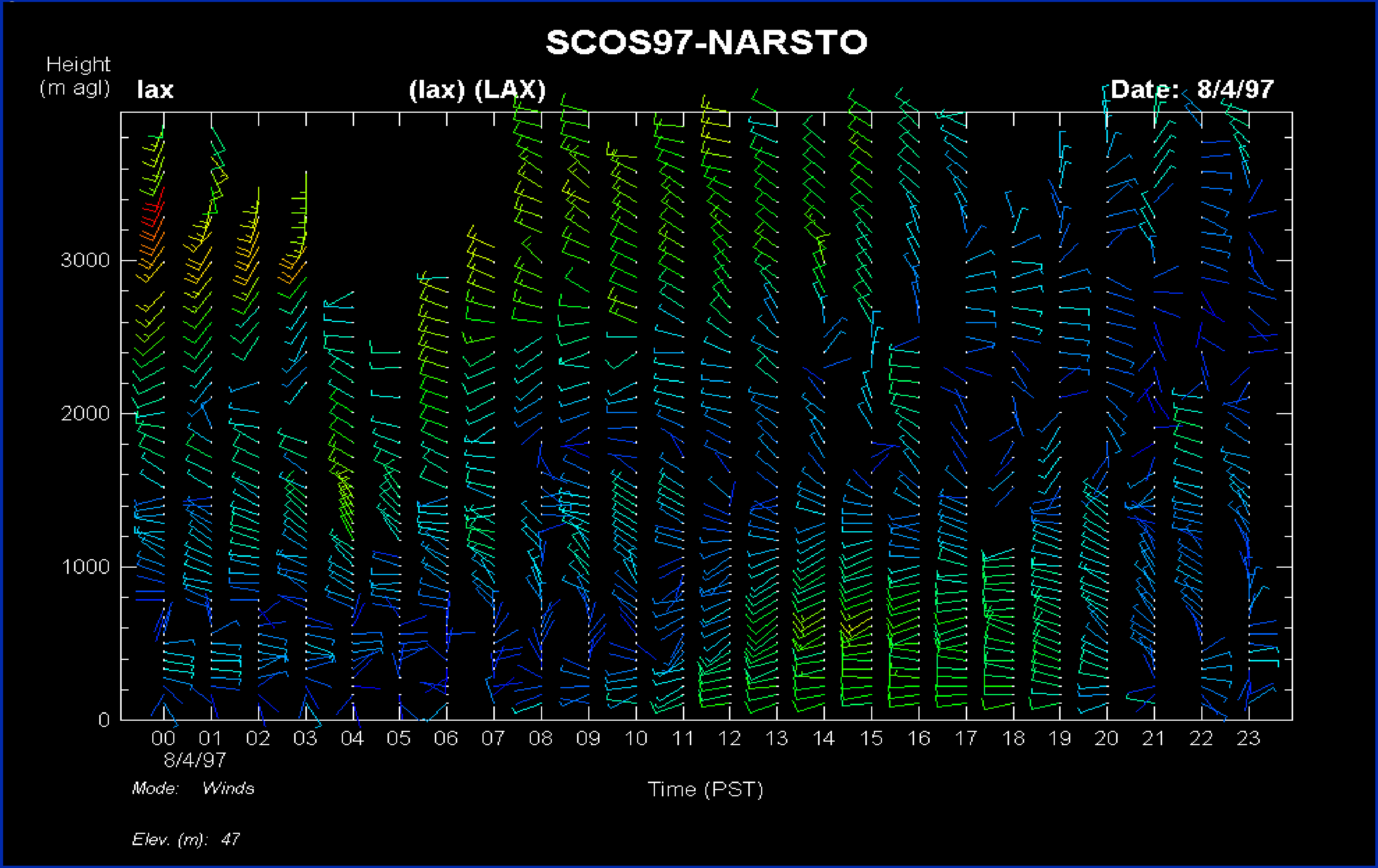

Background – RASS T_v

4 a.m. and 4 p.m. rawinsonde soundings do not capture the onset of the sea breeze

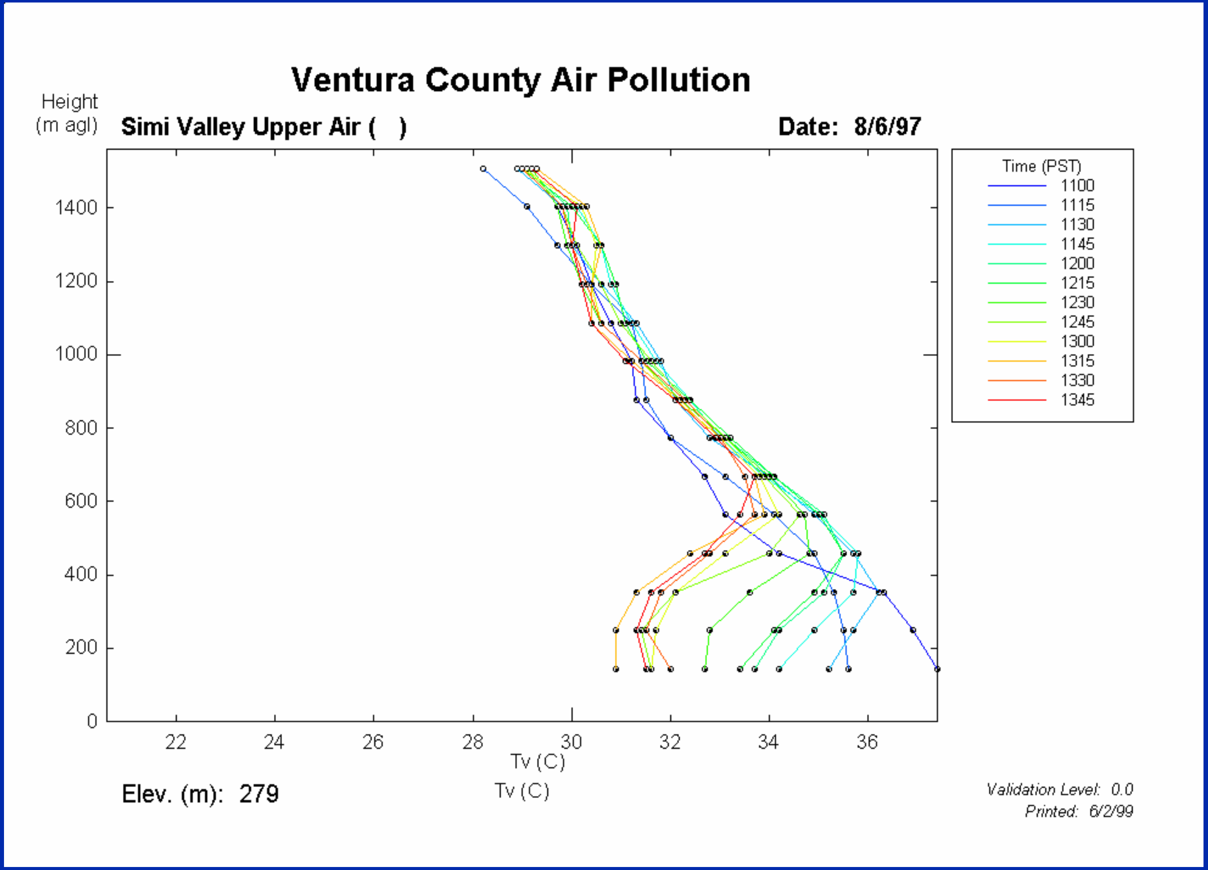

RASS virtual temperature (T_v) data at Simi Valley on August 6, 1997, depicting the onset of the sea breeze

Background – Mixing Derived by Rawinsondes

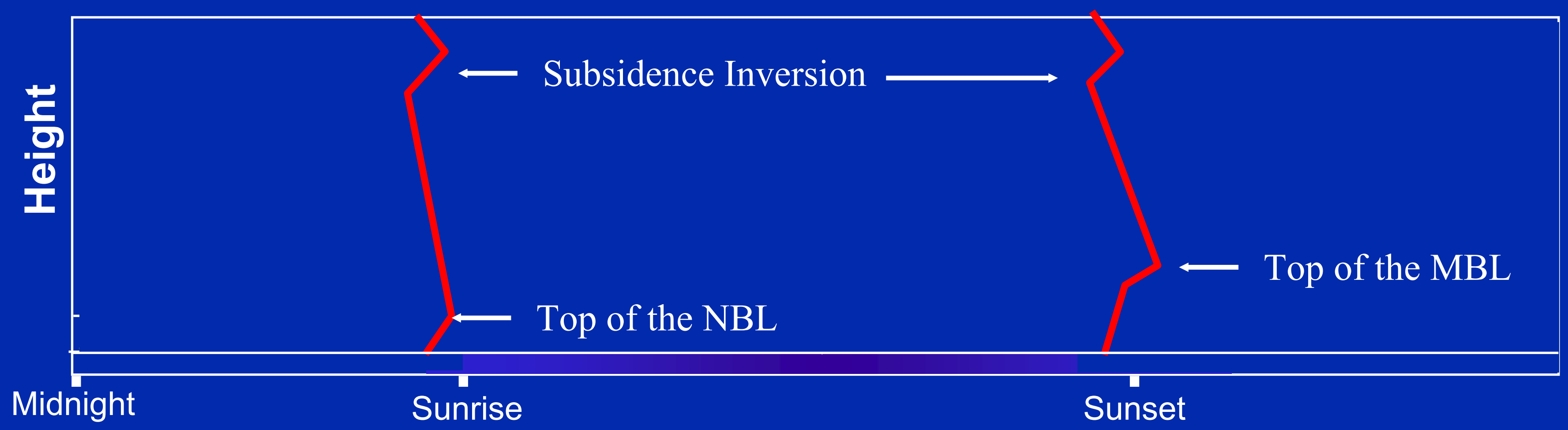

NBL = Nocturnal Boundary Layer
MBL = Marine Boundary Layer

Background - Mixing Derived by RWP and RASS

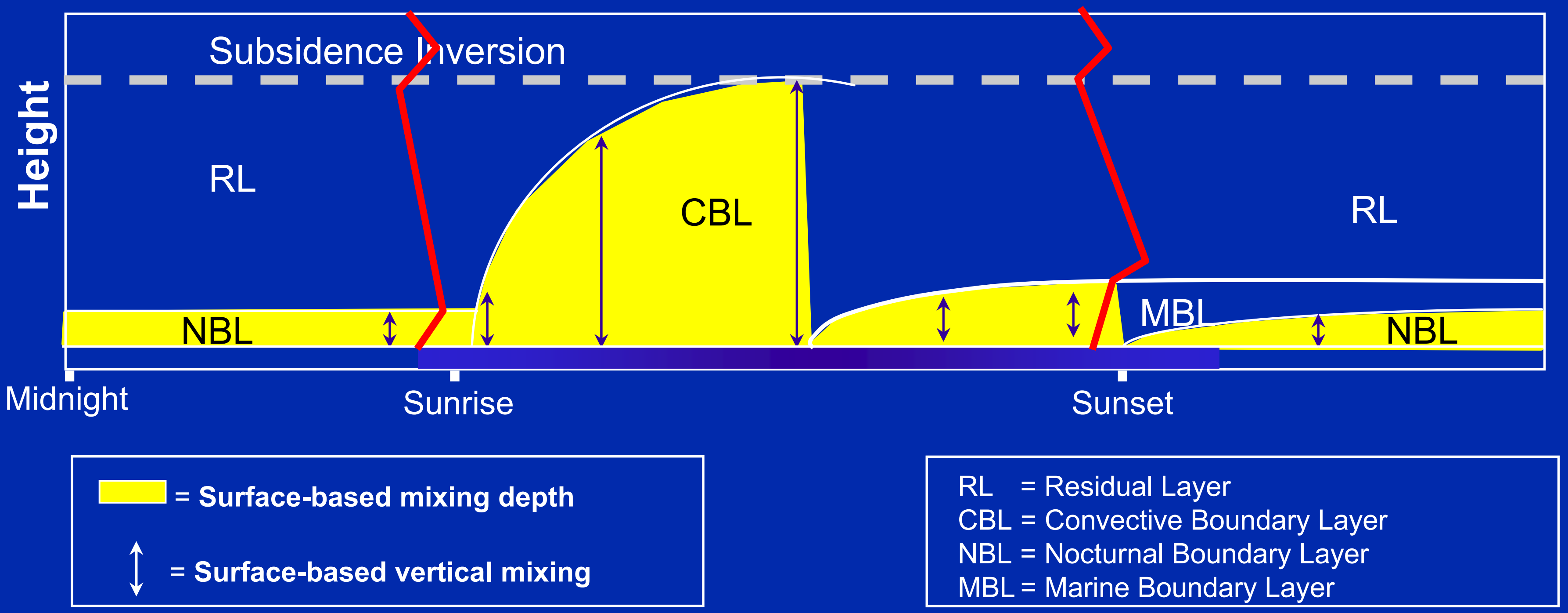

Background – Transport Derived by RWP

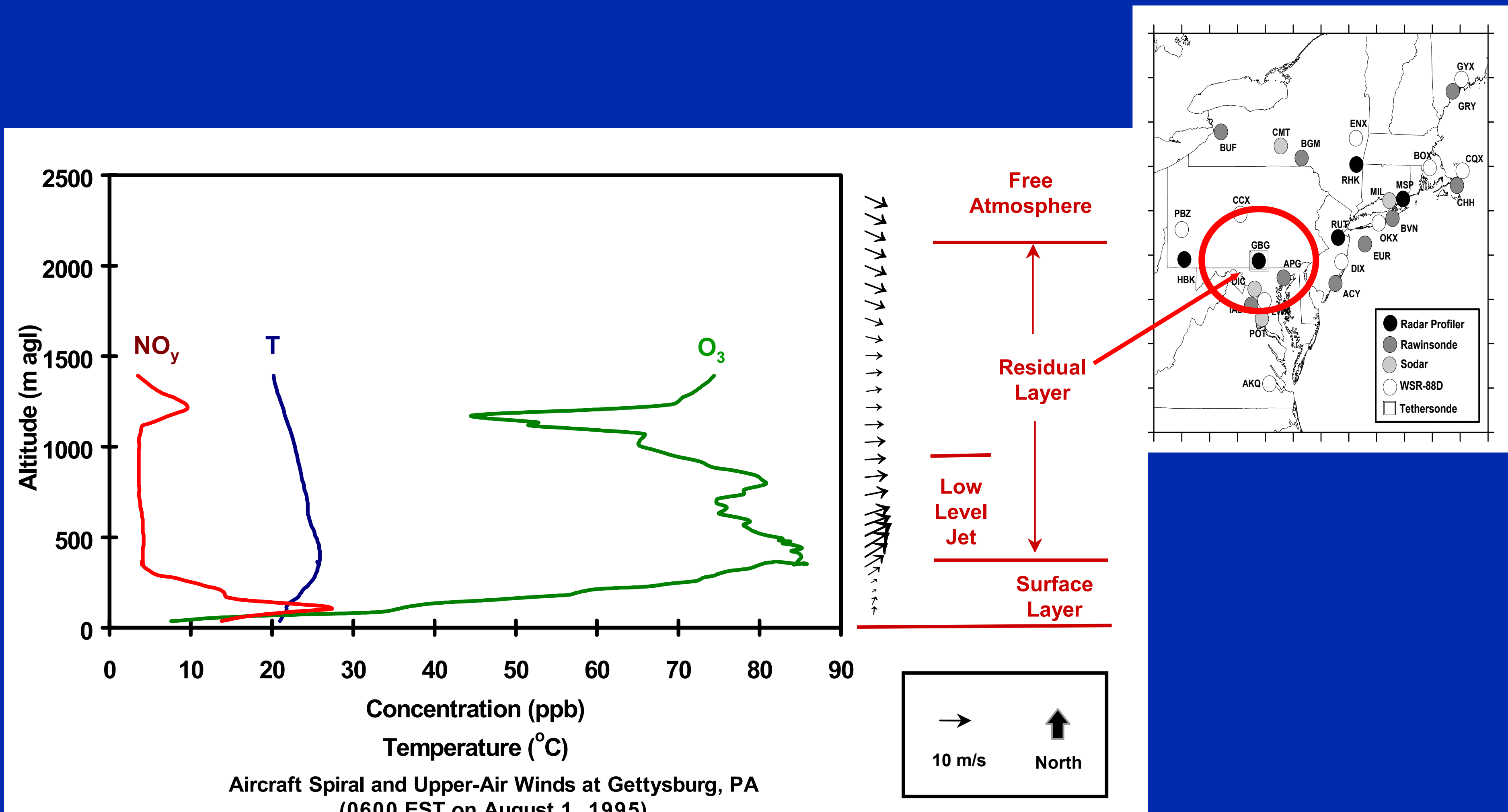

Mixing Depth – Data and Methods

- Mixing depth is the maximum height to which pollutants emitted near the surface will be mixed.
- Mixing depths can be determined using a variety of RWP, RASS and Sodar data:
  - RWP
    - Reflectivity (Cn^2,SNR)
    - Vertical velocity (*w*)
    - Spectral width
    - Horizontal winds
  - RASS
    - Tv profiles
  - Sodar
    - Reflectivity
    - Winds

Mixing Depth – Data and Methods

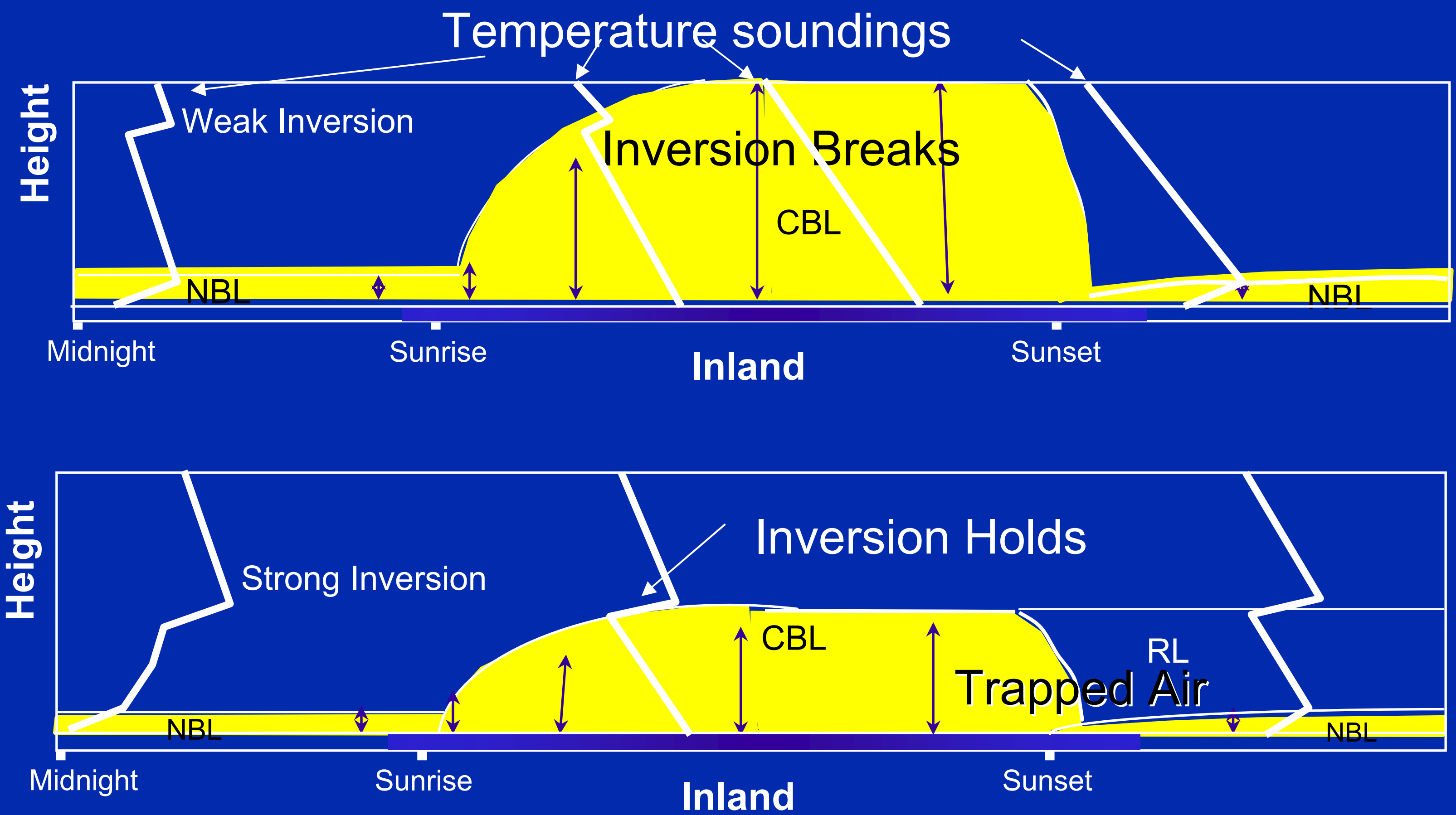

RL = Residual Layer
CBL = Convective Boundary Layer
NBL = Nocturnal Boundary Layer

= Surface-based mixing depth
= Surface-based vertical mixing

Mixing Depth – Data and Methods RWP (1 of 3)

- Reflectivity
  - Measures variations in the refractive index of the atmosphere
  - Turbulence produces variations in atmospheric temperature, humidity, and pressure, which in turn cause variations in the refractive index.
  - Reflectivity largest at inversion capping convective boundary
  - CBL height-finding algorithms – (Angevine et al., 1994; Dye et al., 1995; Bianco and Wilczak, 2002)

Mixing Depth – Data and Methods RWP (2 of 3)

- Vertical Velocity
  - The radial velocity measured by the RWP vertical beam is a direct measure of vertical velocity
  - Convective thermals within the CBL act to vertically redistribute heat, moisture, and momentum
  - Identify the vertical extent of convective thermals to obtain an estimate of mixing depth
- Spectral Width
  - Illustrates the range of radial velocities measured within the scatter volume
  - Locating the gradient in the spectral width (variability in the scales of turbulence) can be used as a reasonable estimate of mixing depth

Mixing Depth – Data and Methods RWP (3 of 3)

Estimating Mixing Depths

Cn^2

Vertical Velocity

Spectral Width

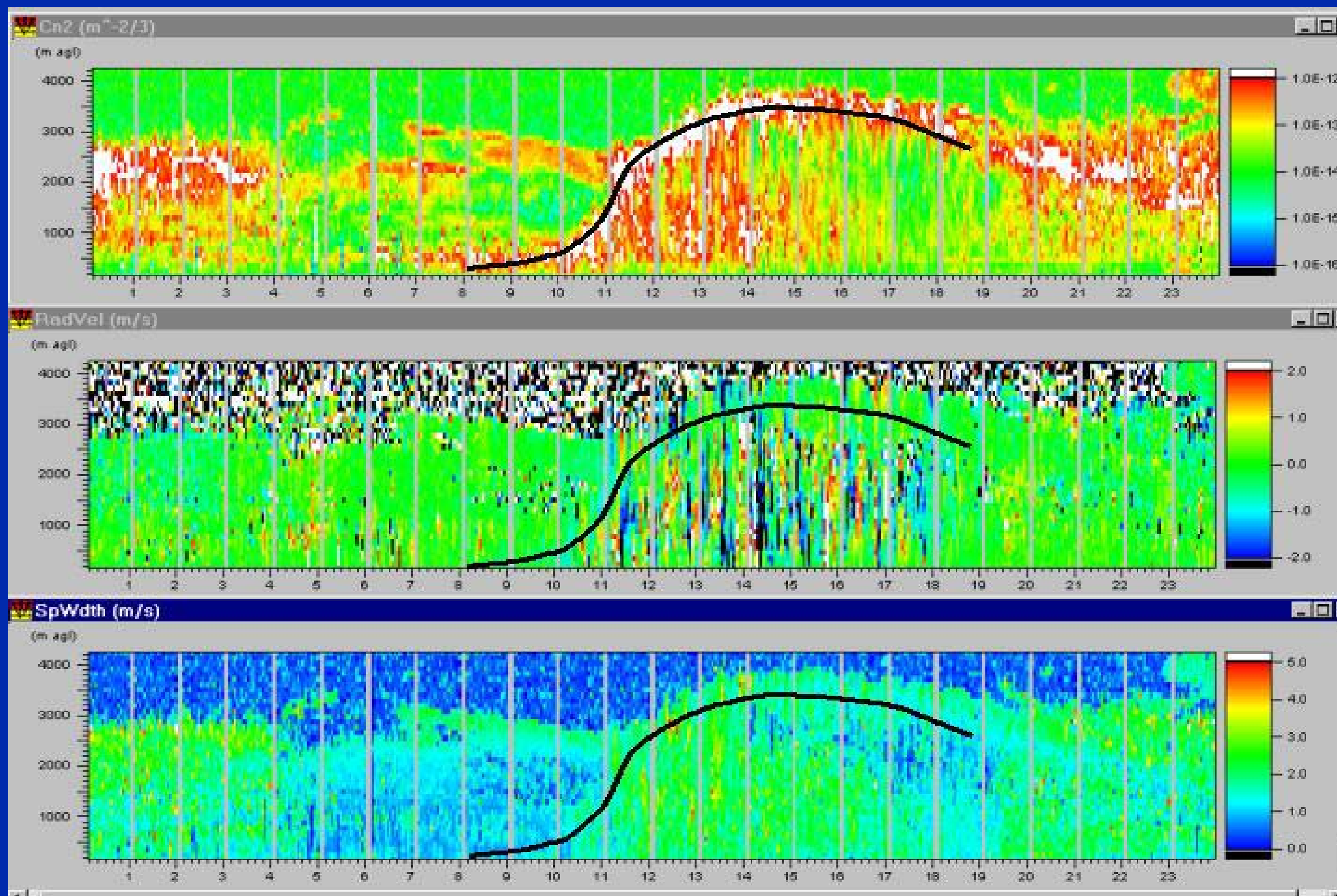

Mixing Depth – Data and Methods RASS (1 of 2)

- Nighttime
  - Inflection point on morning T_v profiles corresponds with maximum height of nocturnal boundary layer (may be higher than true extent of mixing)
- Daytime
  - Point where the surface temperature lifted dry adiabatically intersects with the T_v profile is typically a reasonable estimate of daytime mixed layer height
- Inversion Strength
  - Strength of nocturnal inversion influences the time at which the evolving CBL mixes with the residual layer
  - Strength of the subsidence inversion controls CBL growth

Mixing Depth – Data and Methods RASS (2 of 2)

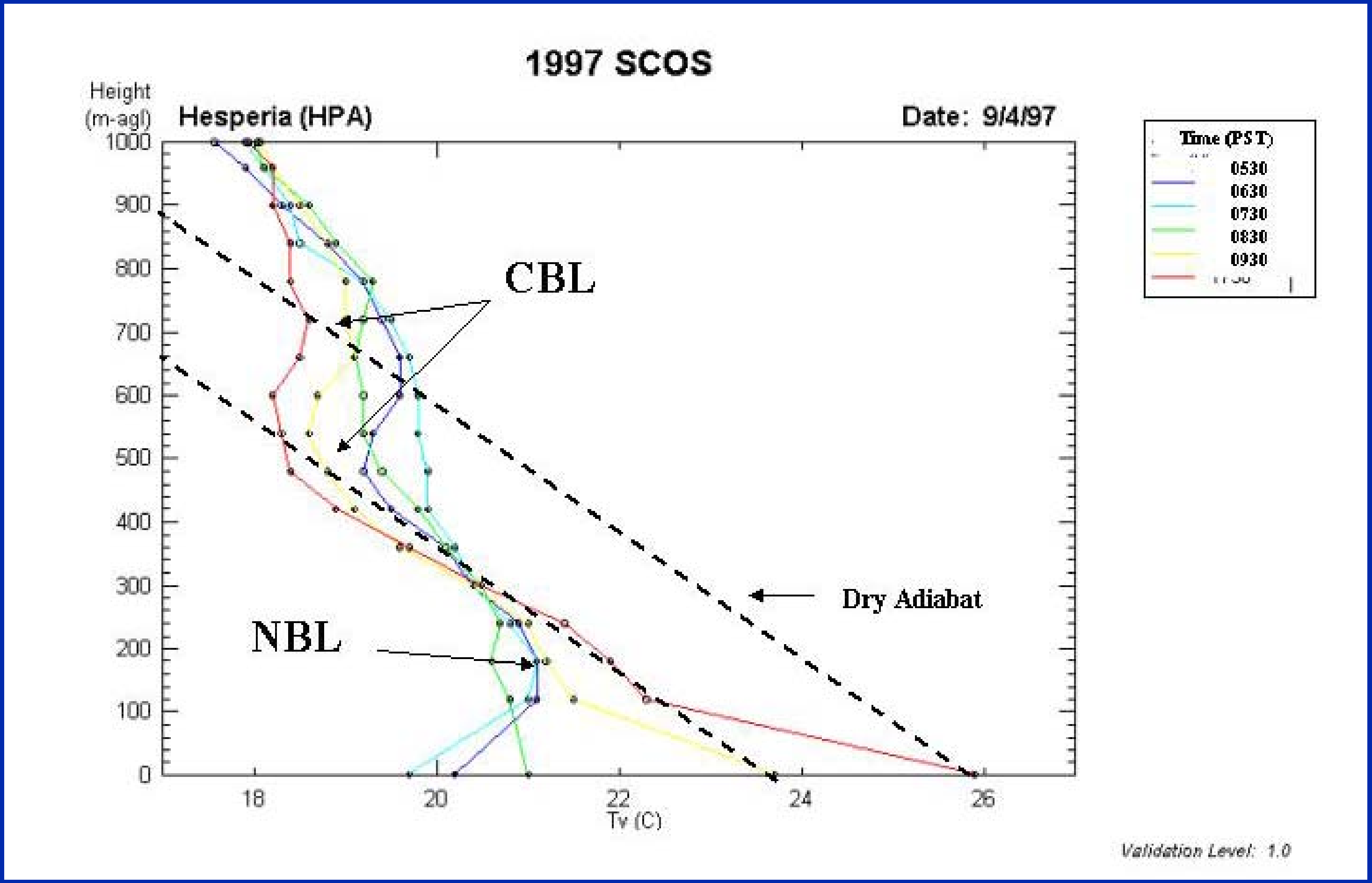

SCOS-97 RASS virtual temperature (T_v) profiles, Hesperia, September 4, 1997

Mixing Depth – Data and Methods RWP Winds (1 of 2)

- During the daytime (CBL), wind profiles will increase with height throughout the surface layer (below first profiler gate), before showing little change throughout the depth of the ABL and, finally, an increase in wind speed above the ABL

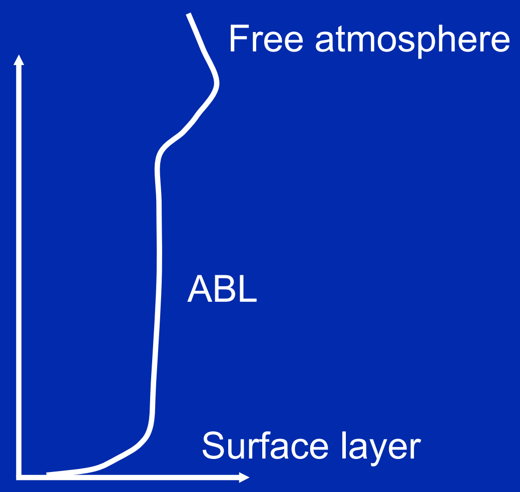

- At night (NBL), an increase in wind speed is typically observed near the top of the NBL as air above the NBL decouples from the surface

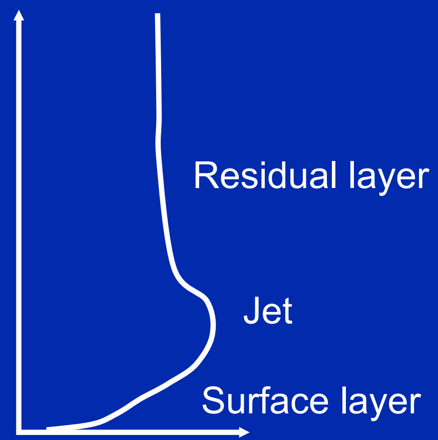

Mixing Depth – Data and Methods RWP Winds (2 of 2)

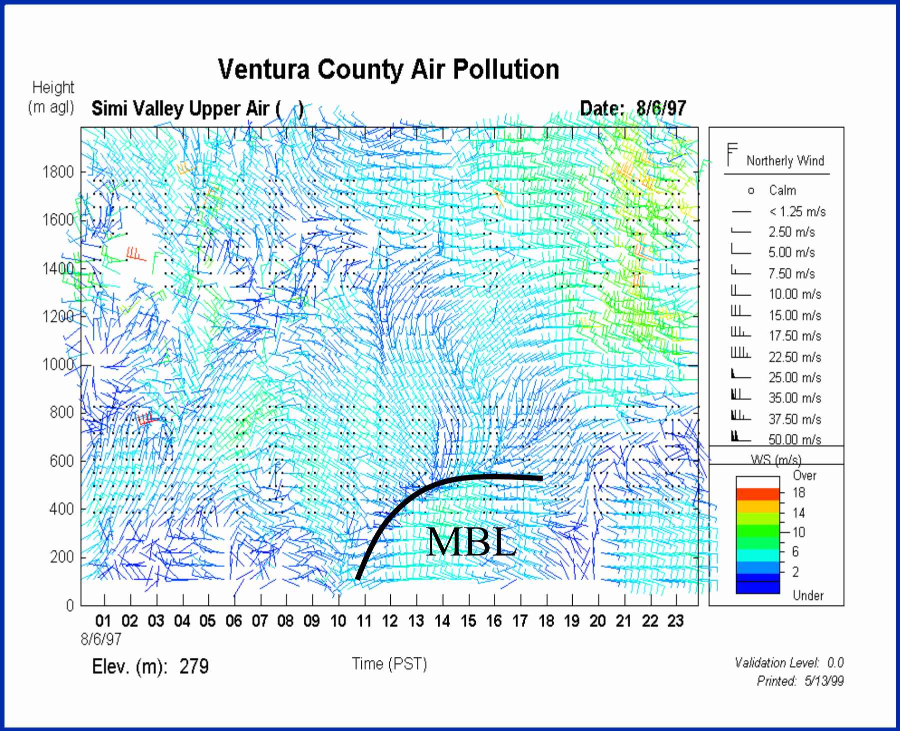

Radar profiler wind data at Ventura on August 6, 1997 showing the sea breeze (MacDonald et. al., 1999)

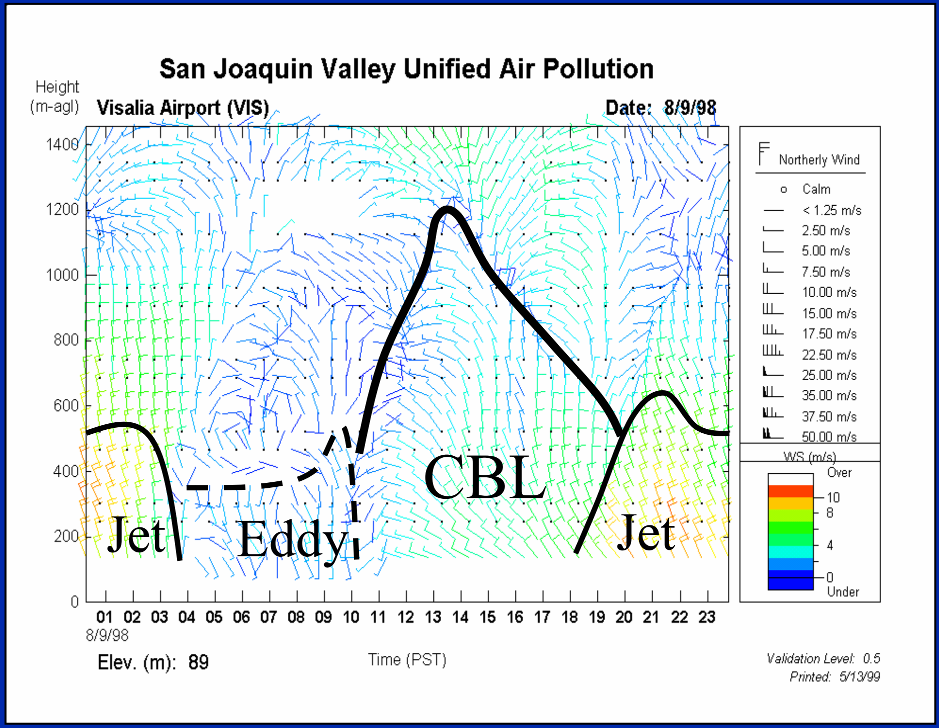

Radar profiler wind data at Visalia on August 9, 1998, showing the nocturnal jet, CBL, and eddy flow. This wind pattern was observed on the majority of the episode days (MacDonald et. al., 1999).

Mixing Depth – Data and Methods Sodar (1 of 2)

Reflectivity – measures variations in the refractive index of the atmosphere (C_T^2)

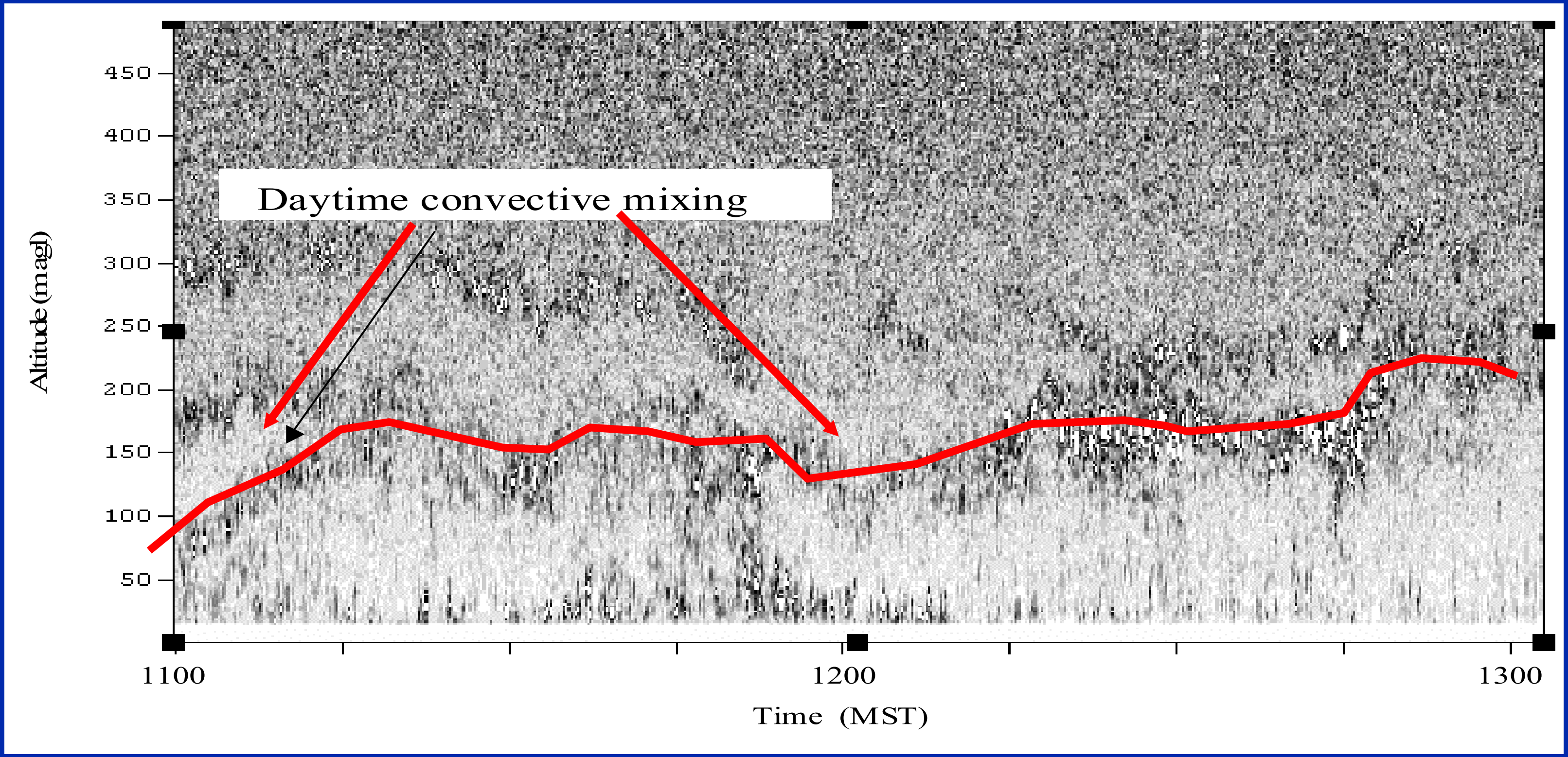

Sodar reflectivity data at Brighton on January 14, 1997, showing the onset of daytime convective mixing (Watson et. al., 1998)

Mixing Depth – Data and Methods Sodar (2 of 2)

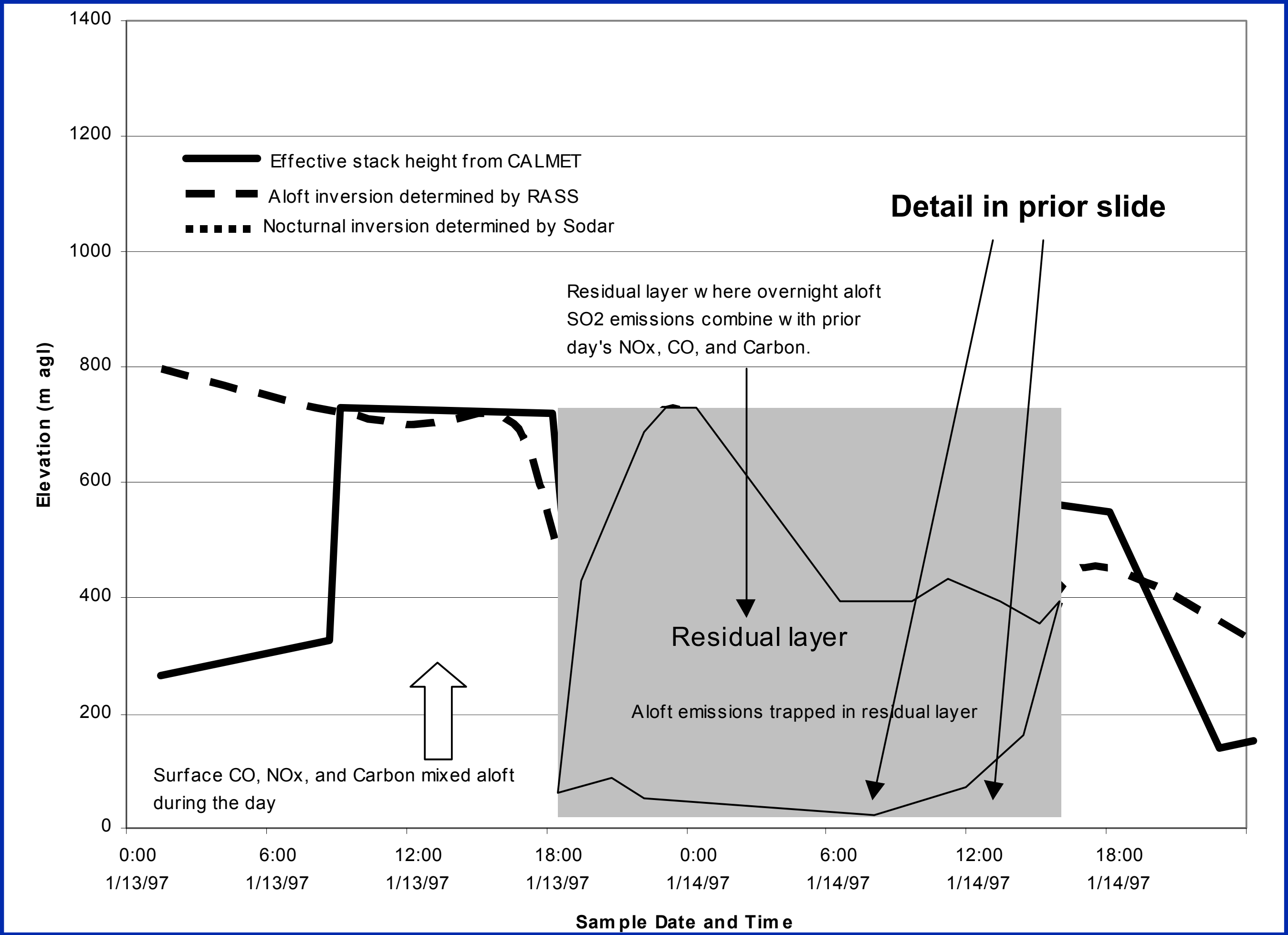

Time series of inversions at Brighton and effective stack heights for the Cherokee and Pawnee stacks on January 13 and 14, 1997 (Watson et. al., 1998)

Mixing Depth – Applications

- Mixing Depth Growth Rate (MGR)
- Peak mixing depth
  - Time of peak mixing depth
- Averaging techniques
- Spatial views (profiler networks)

Mixing Depth – Applications MGR (1 of 5)

- The mixing depth growth rate (MGR) is the rate of change of boundary layer height through time

$$MGR = \Delta h/\Delta t$$

  where h is the height of the boundary layer and t is time.
- Rapid CBL evolution occurs between 0600 and 1200 local time and is a good choice for Δt
- MGR is important because it indicates the rate of change in the volume of air in which pollutants mix and indicates rate of entrainment of aloft air
- MGR is controlled by aloft stability and the partitioning of solar radiation between the sensible and latent heat flux at the surface

Mixing Depth – Applications MGR (2 of 5)

1996 Paso del Norte Summer Ozone Study

August 12, 1996

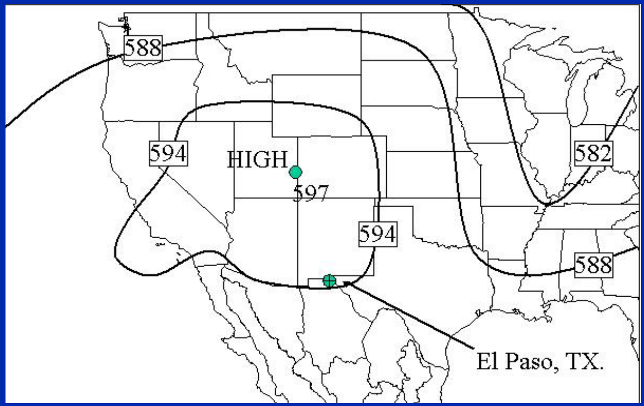

August 13, 1996

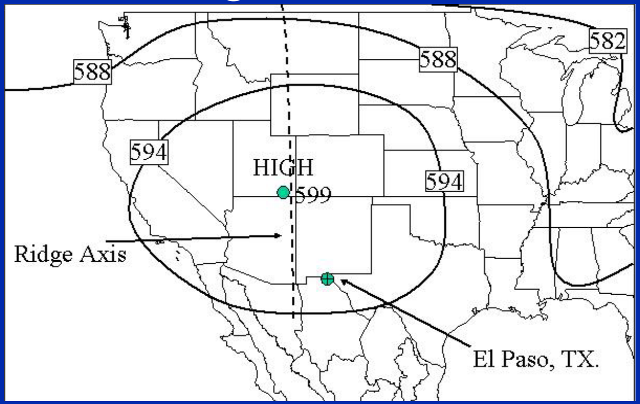

August 14, 1996

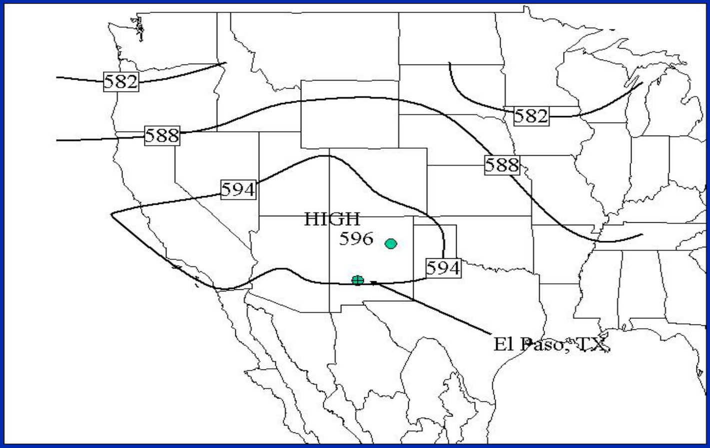

500-mb Heights at 1700 MST for August 12 through August 14, 1996 (MacDonald et al., 2001a)

Mixing Depth – Applications MGR (3 of 5)

1996 Paso del Norte Summer Ozone Study

Morning inversion increased from 6.5°C on August 12 to 8.7°C on August 13, to 9.7°C on August 14

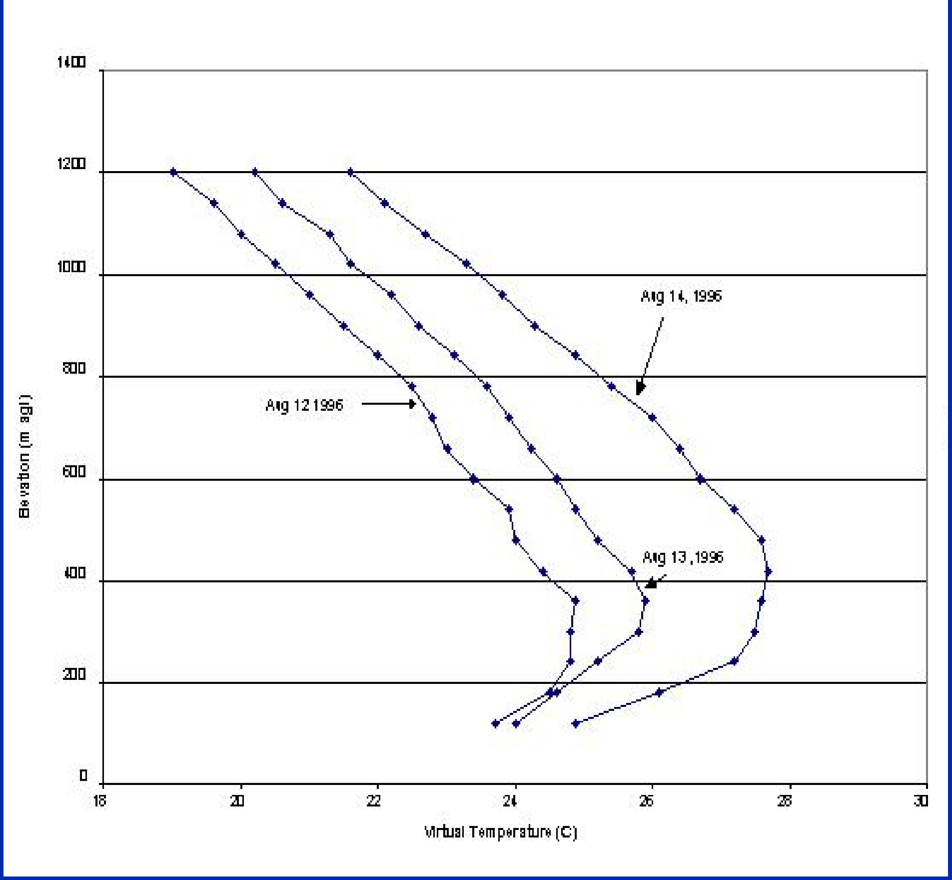

RASS virtual temperature on August 12 through 14, 1996, at 0600 MST (MacDonald et al., 2001a)

Mixing Depth – Applications MGR (4 of 5)

1996 Paso del Norte Summer Ozone Study

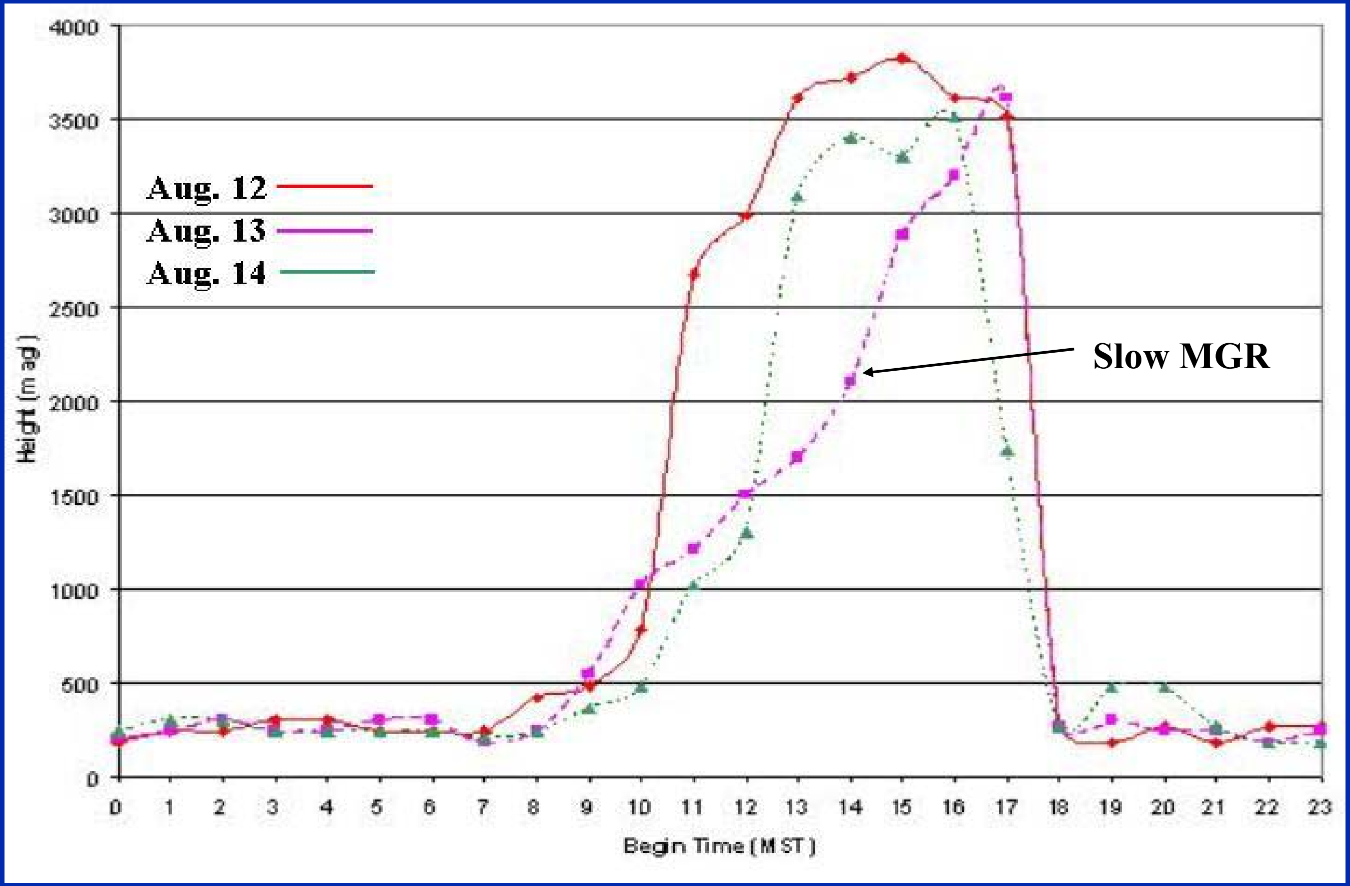

Mixing depths on August 12 through 14, 1996 (MacDonald et al., 2001a)

Mixing Depth – Applications MGR (5 of 5)

1996 Paso del Norte Summer Ozone Study

Summary of Results

Parameter	August 12	August 13	August 14
MGR (m/hr)	380	150	120
Peak Mixing Depth. (m)	3800	3700	3600
Avg. Surface Wind Speed (m/s) (0600-1000, local time)	1.3	0.9	2.0
Peak Ozone (ppb)	77	137	79

A slower MGR and light winds lead to a higher peak ozone value on August 13 (MacDonald et al., 2001a)

Mixing Depth – Applications Peak Mixing (1 of 6)

- The peak mixing depth is the maximum vertical extent of the atmospheric boundary layer
- The peak mixing depth influences air quality concentrations by
  - defining the volume in which pollutants mix
  - influencing chemistry rates
- The timing of this peak depth is also critical
  - The same peak but different time will result in different air quality concentrations

Mixing Depth – Applications
Peak Mixing (2 of 6)

Sacramento, July 16, 1998

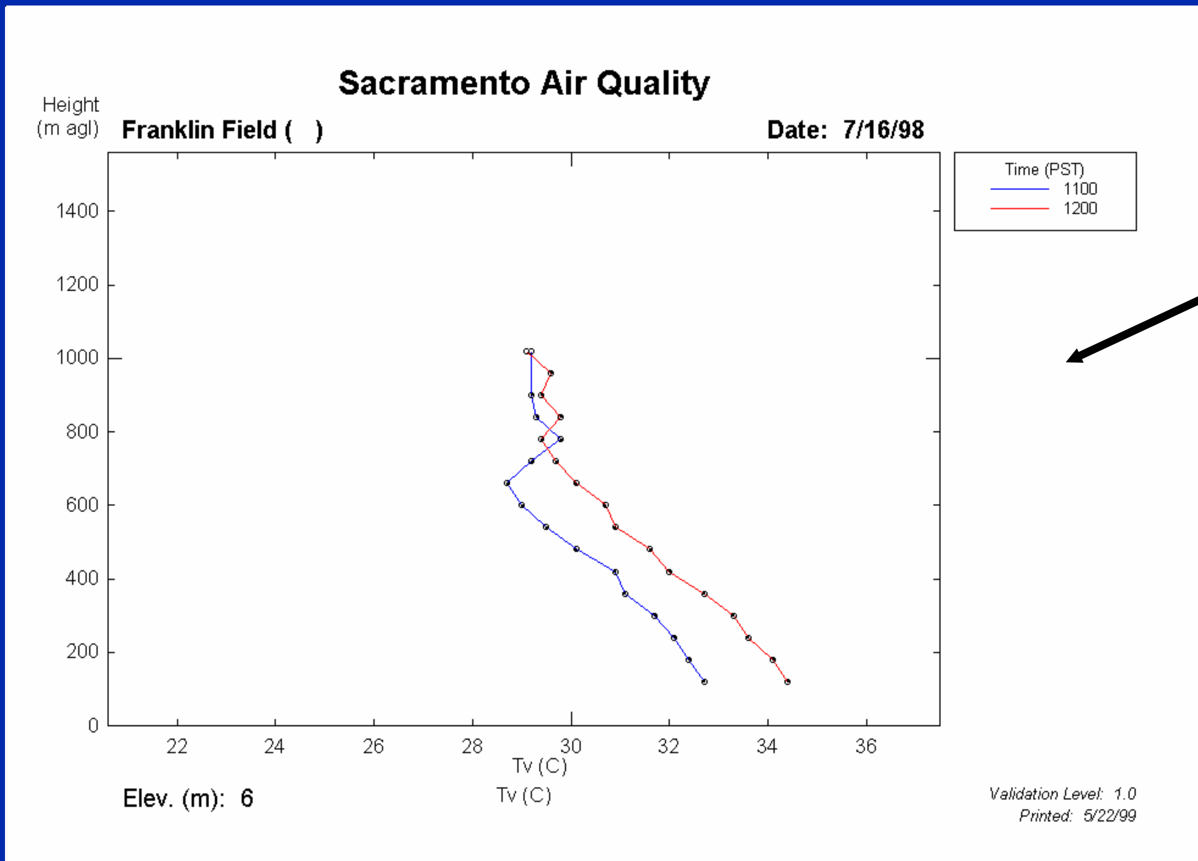

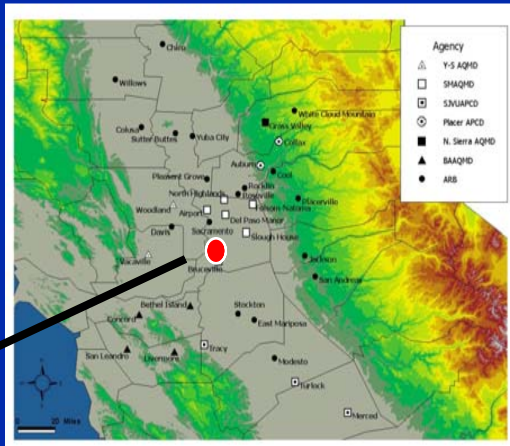

RASS virtual temperature data at Franklin Field on July 16, 1998 showing a subsidence inversion at about 800 m (MacDonald et al., 1999)

Mixing Depth – Applications Peak Mixing (3 of 6)

Sacramento, July 16, 1998

(a)

(b)

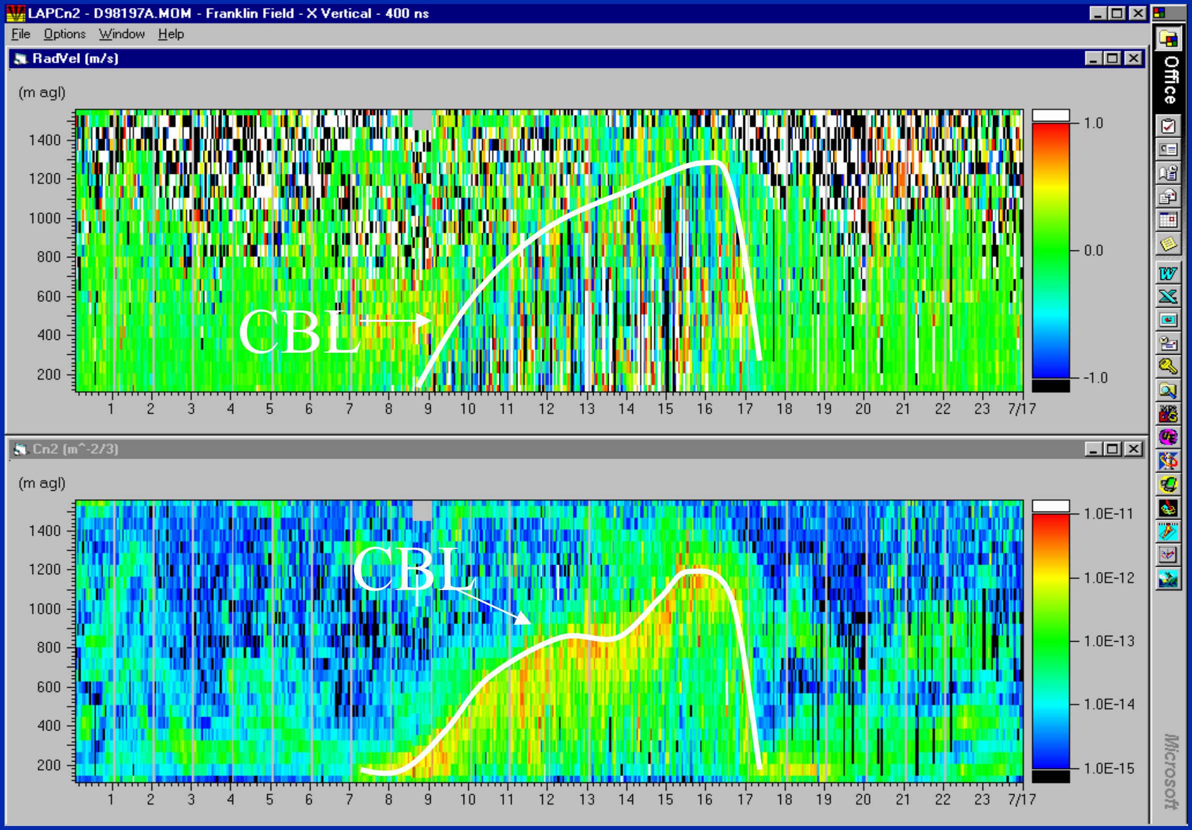

Time (PST)

Time/height cross-section of radar profiler (a) vertical velocity and (b) C_n^2 data at Franklin Field on July 16, 1998. The top of the CBL is shown as a white line (MacDonald et al., 1999)

Mixing Depth – Applications Peak Mixing (4 of 6)

Sacramento, July 17, 1998

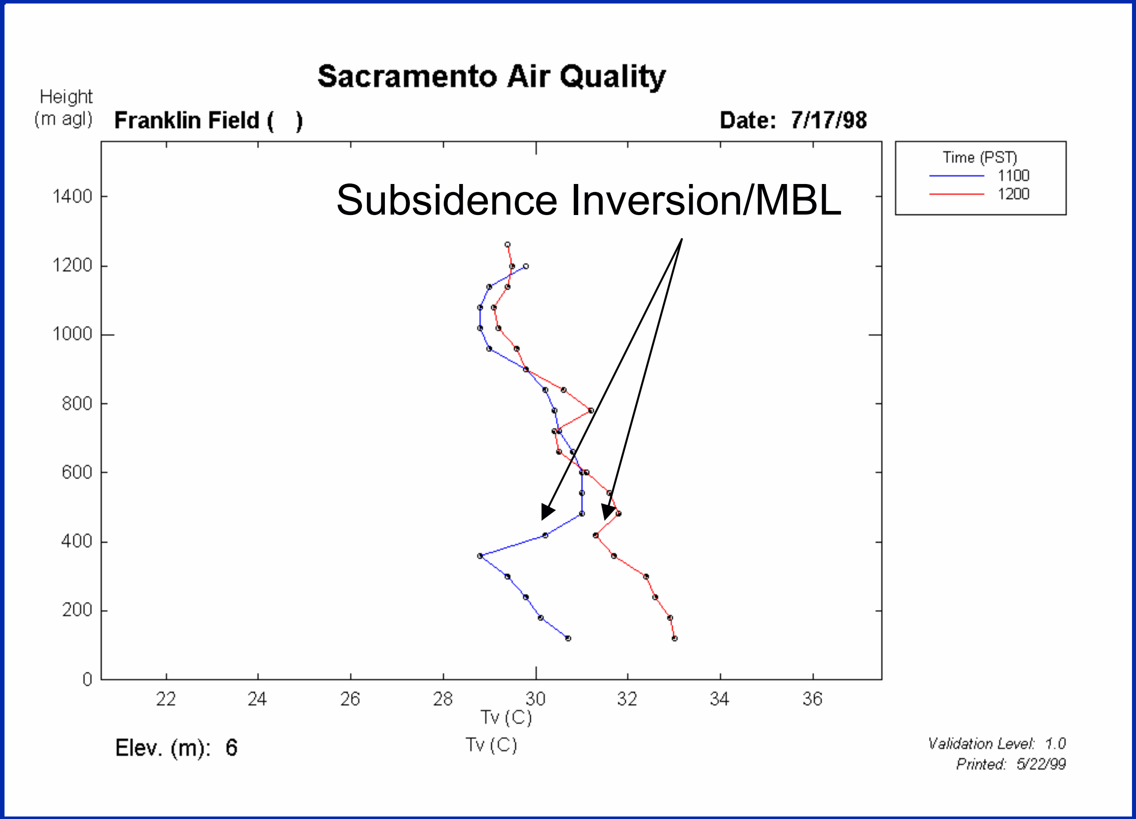

RASS virtual temperature data at Franklin Field on July 17, 1998, showing a subsidence inversion at about 500 m (MacDonald et al. 1999)

Mixing Depth – Applications Peak Mixing (5 of 6)

Sacramento July 17, 1998

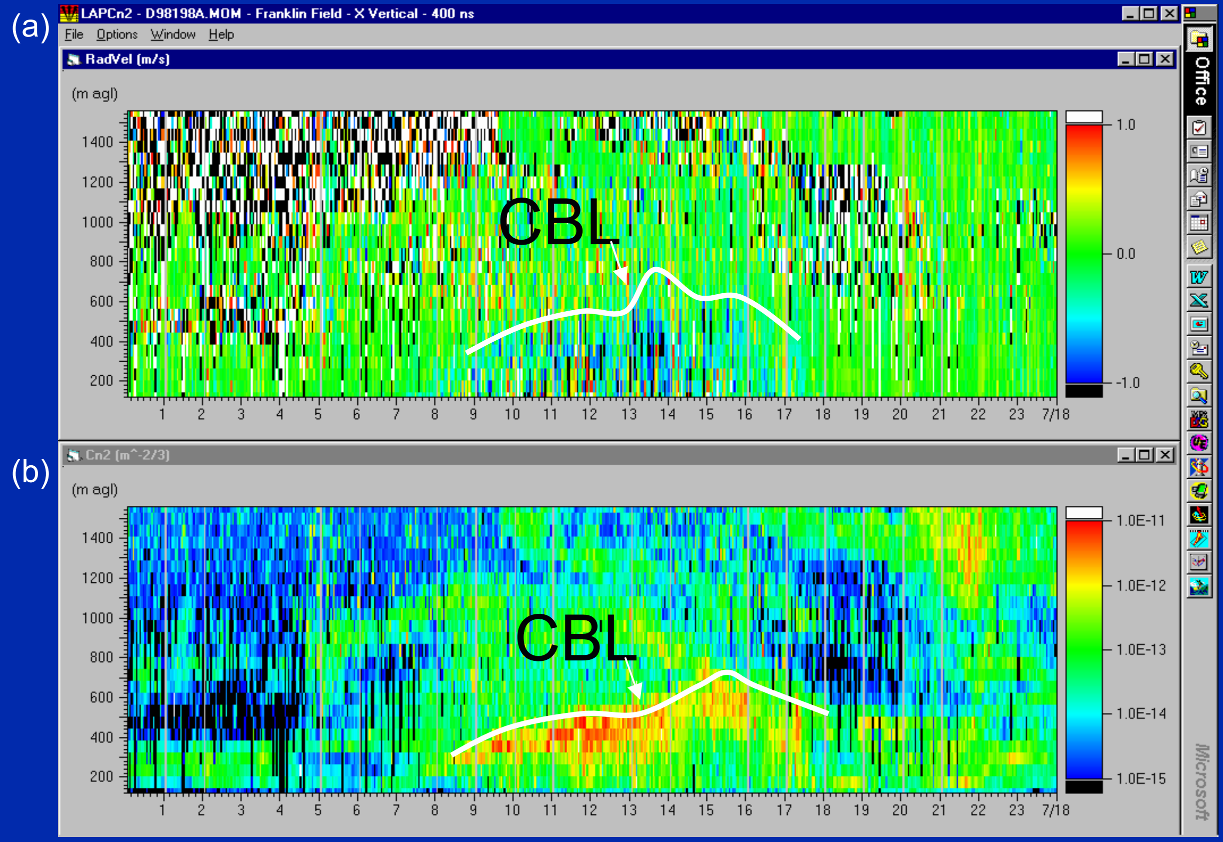

Time (PST)

Time/height cross-section of radar profiler (a) vertical velocity and (b) C_n^2 data at Franklin Field on July 17, 1998. The top of the CBL is shown as a white line (MacDonald et al., 1999).

Mixing Depth – Applications Peak Mixing (6 of 6)

Sacramento, July 16-17, 1998

- Broad upper-level high over California
- Warm aloft temperatures
- Shallower mixing depths on the July 17 compared to July 16

Ozone	July 16	July 17
1-hour max (ppb)	95	137
8-hour avg (ppb)	120	152

Mixing Depth – Applications Averaging Techniques (1 of 6)

- Average mixing depth, winds, and T_v
- Helps to view the “forest through the trees”
- Group by
  - Flow types
  - Episode vs. non-episode
  - Synoptic classification (ridge, trough, cut-off low, etc.)
  - Seasons
  - Years
  - Months

Mixing Depth – Applications Averaging Techniques (2 of 6)

Mean Seasonal T_v Profiles

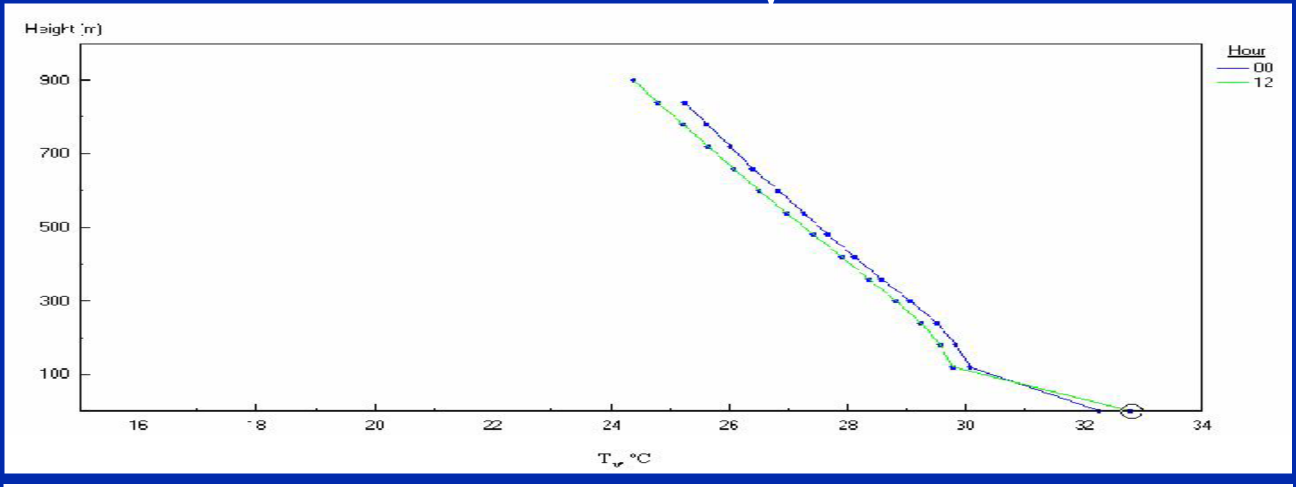

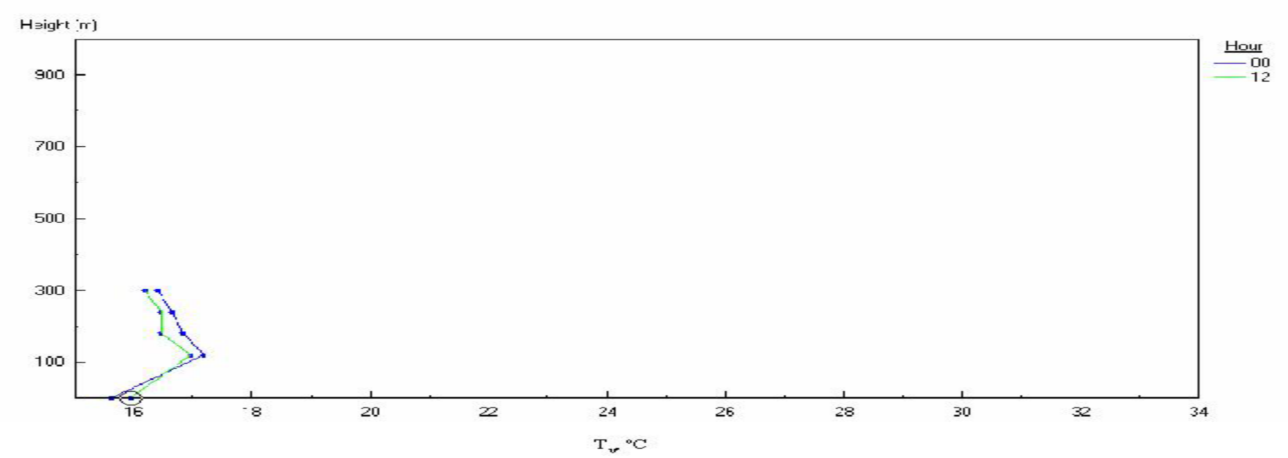

- Average each gate for nighttime and daytime
- Set minimum percent needed (e.g., 50%)

Average daytime and nighttime RASS T_v data over the Gulf of Mexico at Vermillion during the summer (top) and winter (bottom) (MacDonald et al., 2002)

Mixing Depth – Applications Averaging Techniques (3 of 6)

Annual Wind Profiles

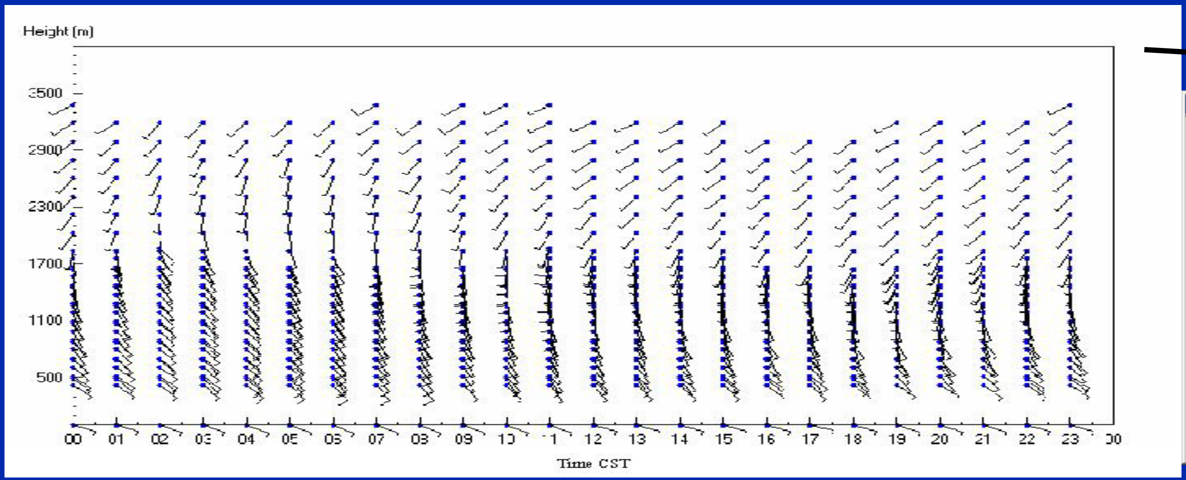

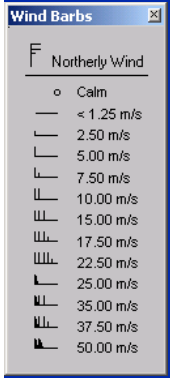

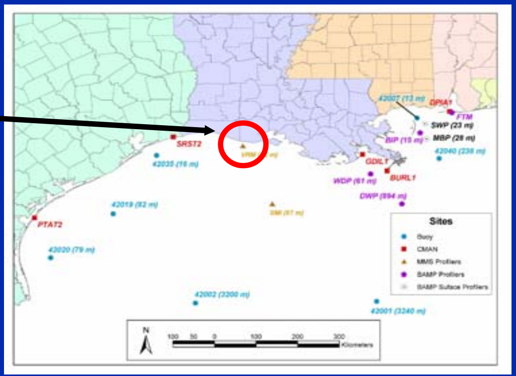

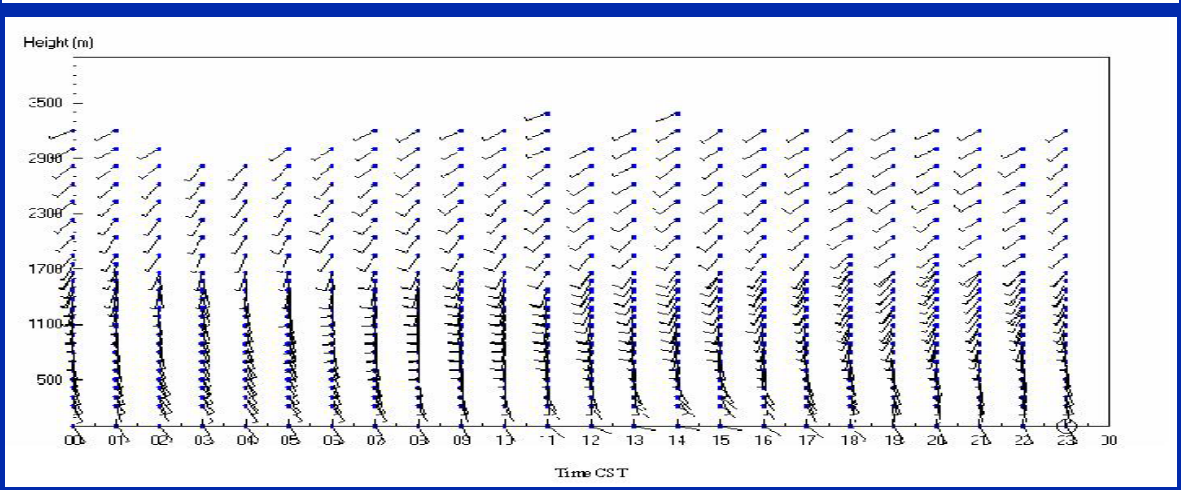

- Average each gate for each hour
- Set minimum percent needed (e.g., 50%)

1998 average radar profiler wind data over the Gulf of Mexico at South Marsh Island (top) and Vermillion (bottom) (MacDonald et al., 2002)

Mixing Depth – Applications Averaging Techniques (4 of 6)

Mean Winds by Synoptic Pattern

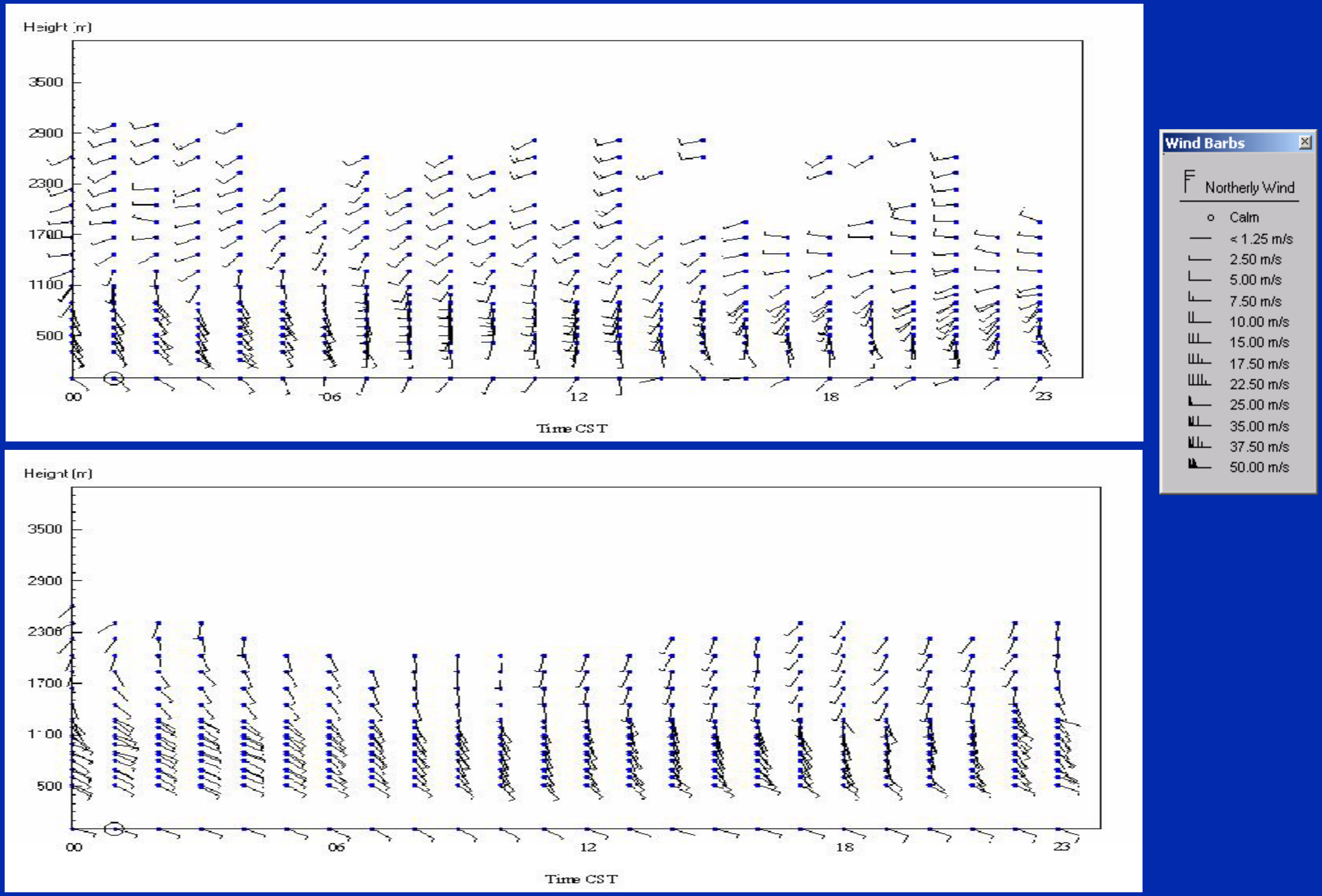

Average radar profiler wind data over the Gulf of Mexico at Vermillion during a trough pattern (top) and ridge pattern (bottom), (MacDonald et al., 2002)

Mixing Depth – Applications
Averaging Techniques (5 of 6)

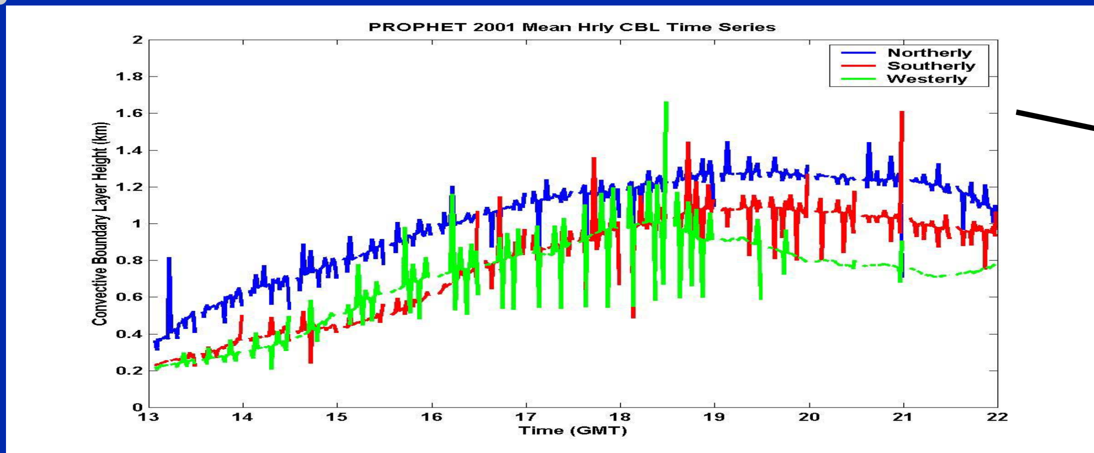

PROPHET July and August 2001 hourly running mean mixing depths categorized by synoptic transport (13Z-22Z)

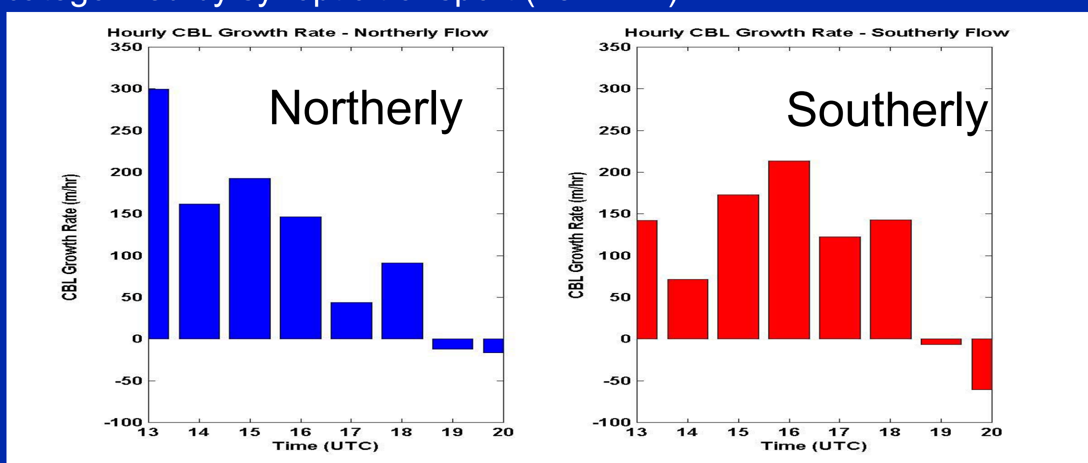

PROPHET 2001 Mean MGR categorized by synoptic transport (13Z-20Z)

- CBL heights measured during northerly flow are ~200 m higher than CBL heights measured during southerly flow
- MGRs measured during northerly flow are twice as great as MGRs during southerly flow from 0900 to 1000 EDT (1300 to1400 UTC)

(Lilly, 2003)

Mixing Depth – Applications Averaging Techniques (6 of 6)

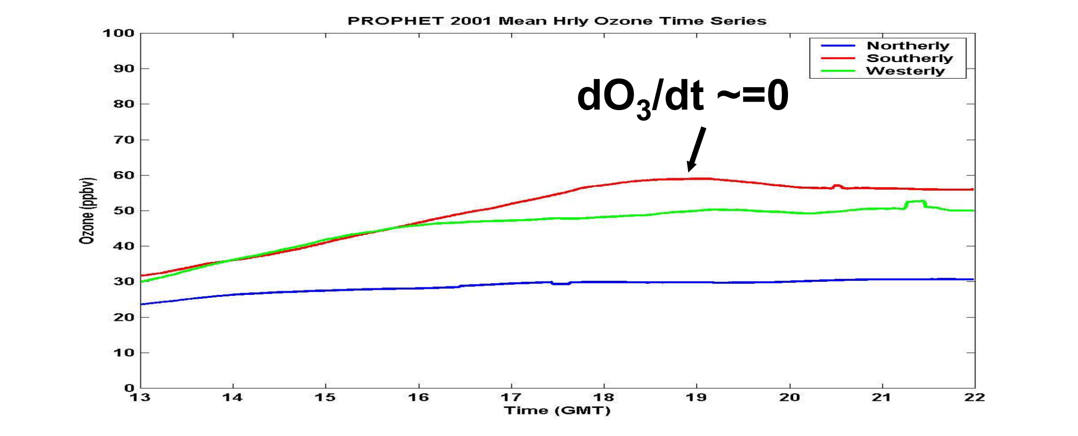

PROPHET 2001 mean ozone time series categorized by synoptic transport, 0900–1800 EDT (13Z-22Z)

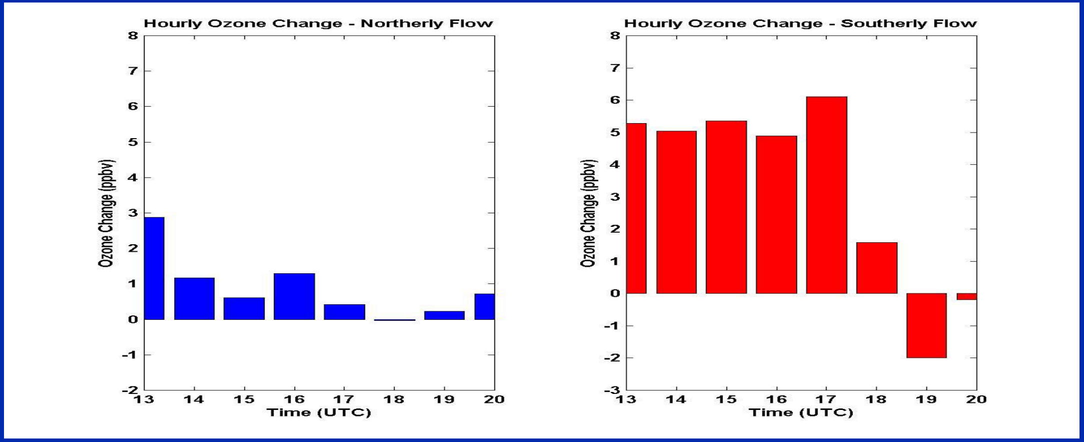

PROPHET 2001 mean hourly ozone change categorized by synoptic transport, 0900–1600 EDT (13Z-20Z)

- At University of Michigan, little local production of ozone occurs; however, the site is dominated by ozone transport.
- A polluted air mass from south is transported into the region and is entrained into the evolving CBL, increasing surface ozone.
- Through the same process, a clean air mass to the north can act to dilute surface ozone (offset any local production).

(Lilly, 2003, in progress)

Mixing Depth – Applications Spatial Views (1 of 6)

- Use network of sites to assess the temporal and spatial variations in mixing, winds, and T_v profiles
- Important because many areas have strong temporal and spatial variations in meteorology, which has a large impact on air quality

Mixing Depth – Applications Spatial Views (2 of 6)

SCOS-97 cross-section of sites

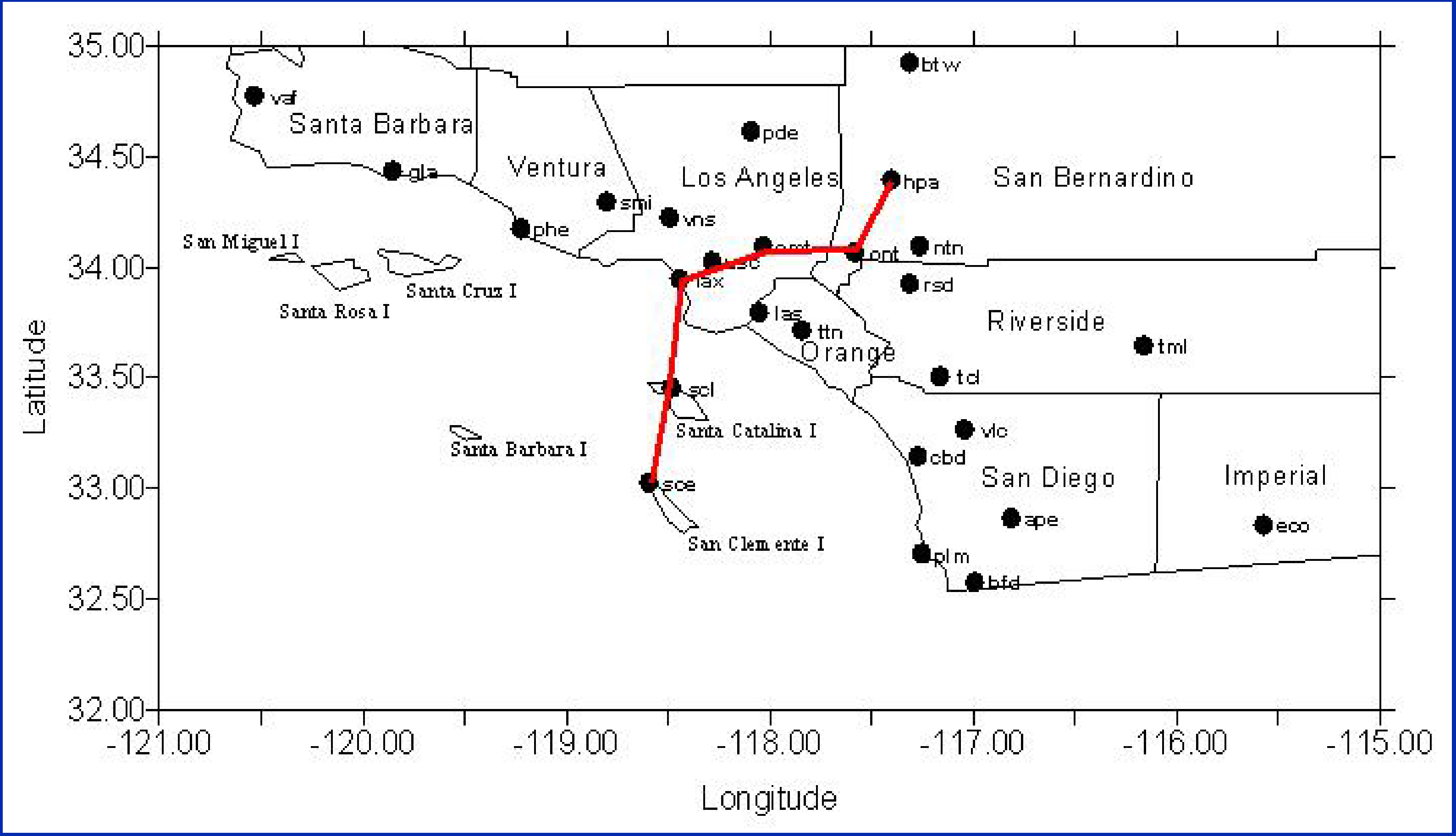

SCOS-97 radar wind profiler and RASS sites (MacDonald et al., 2001b)

Mixing Depth – Applications Spatial Views (3 of 6)

SCOS-97 cross-section of mixing depths, September 4, 1997

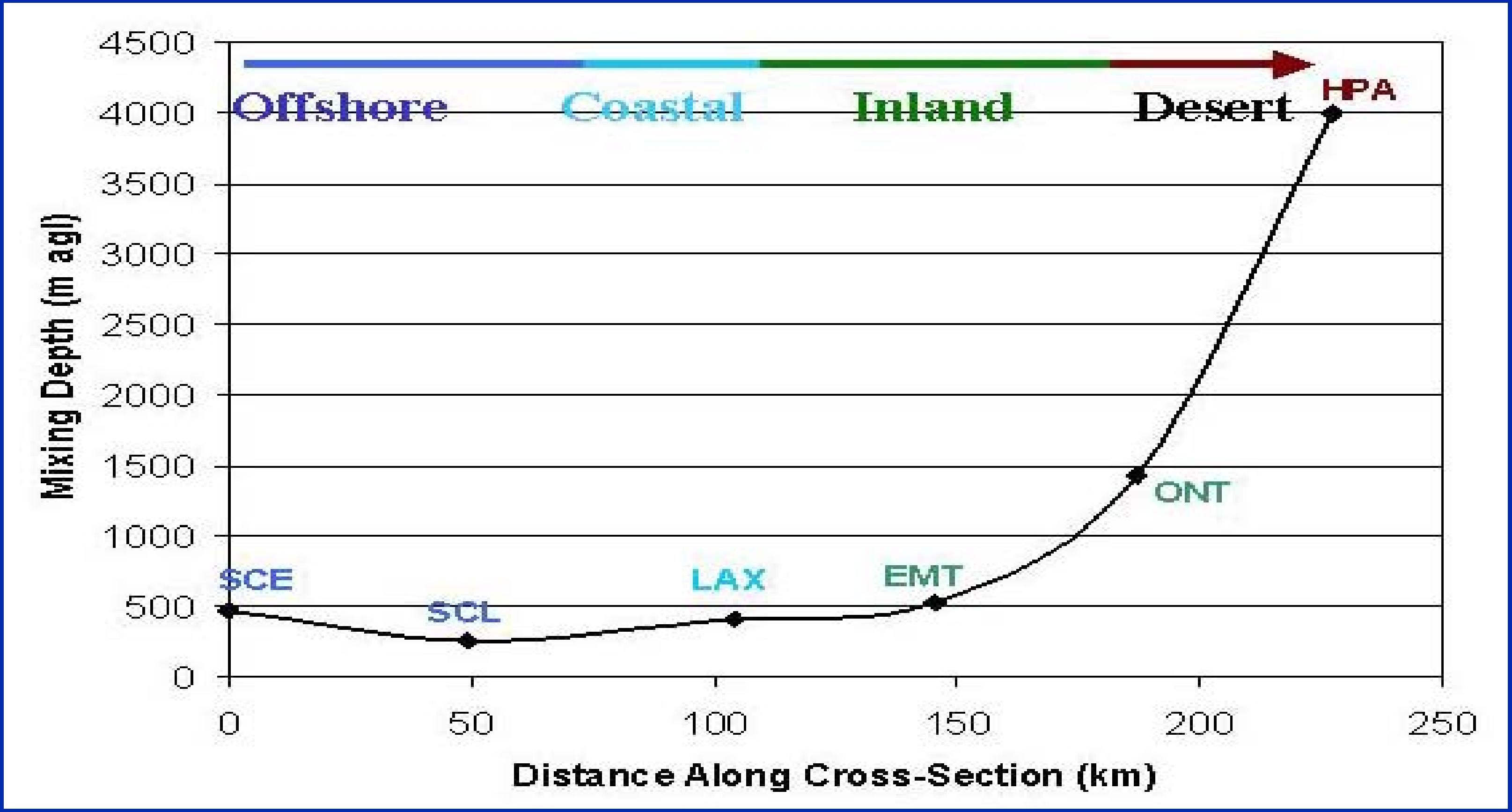

East-to-west cross-section of mixing depths from San Clemente Island (SCE) to Hesperia (HPA) on September 4, 1997, at 1400 PST (MacDonald et al., 2001b)

Mixing Depth – Applications Spatial Views (4 of 6)

SCOS-97 mixing depths, September 4, 1997

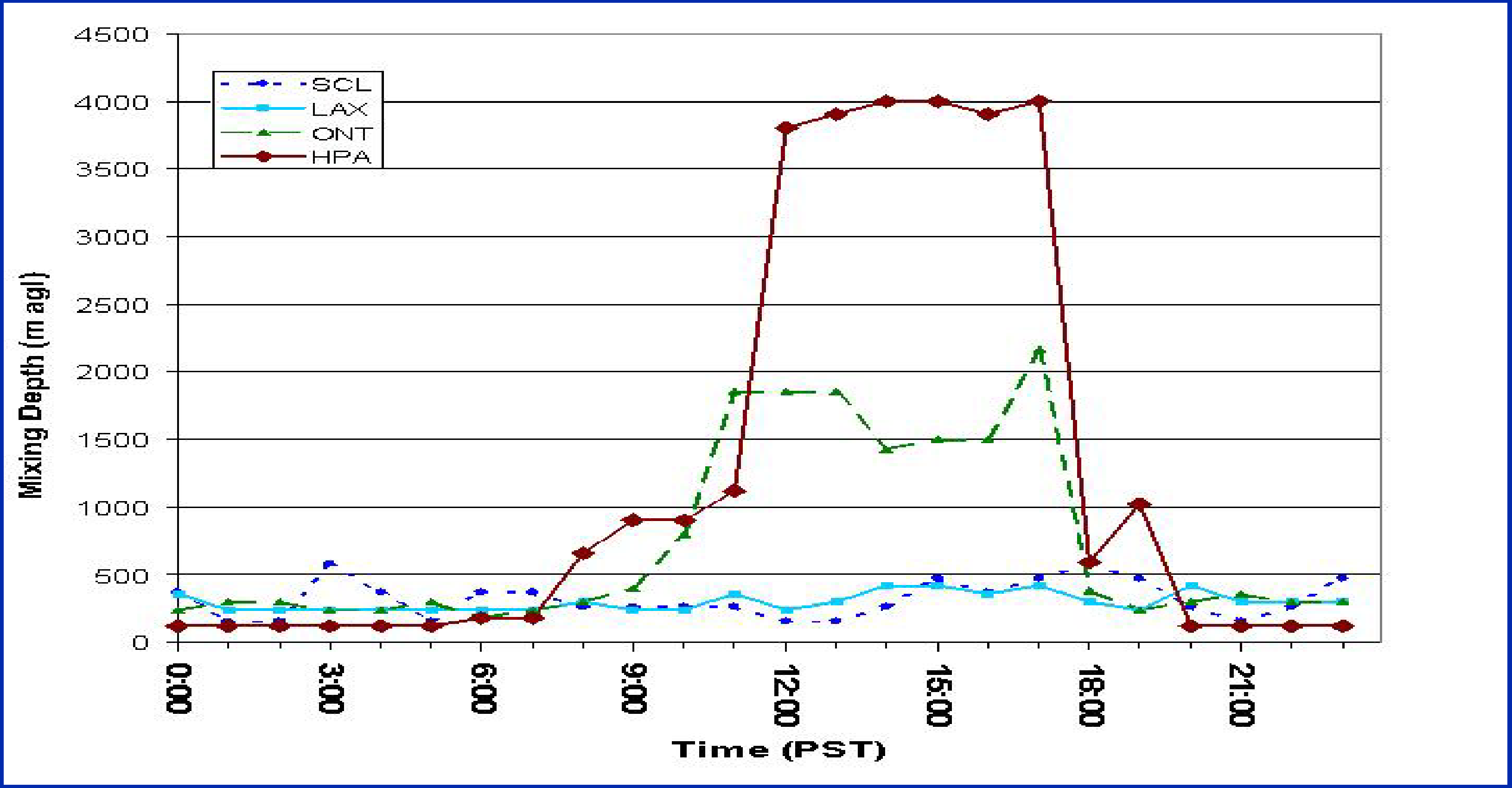

Diurnal cycle of mixing depths on September 4, 1997, at Santa Catalina Island (SCL), Los Angeles Int. Airport (LAX), Ontario (ONT), and Hesperia (HPA) (MacDonald et al., 2001b)

Mixing Depth – Applications Spatial Views (5 of 6)

SCOS-97 mixing depths, September 4, 1997

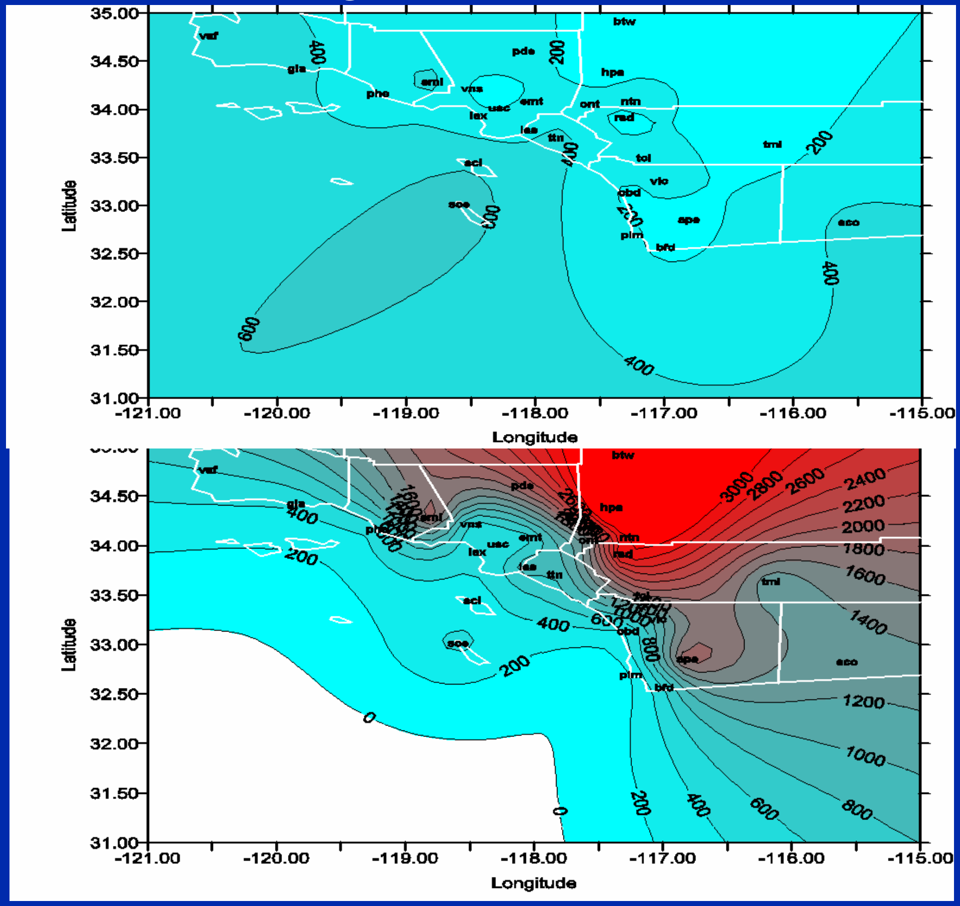

Spatial distribution of mixing depths on September 4, 1997, at 0300 PST (top) and 1400 PST (bottom) (MacDonald et al., 2001b)

Mixing Depth – Applications Spatial Views (6 of 6)

SCOS-97 Summary Results

- Mixing depths at coastal sites were typically about 400 to 600 m agl
- Daily maximum mixing depths at basin sites such as Ontario and Riverside were typically about 1000 to 2000 m agl
- Daily maximum mixing depths at desert sites were typically about 3000 to 4000 m agl but ranged from 1400 to 4000 m agl
- There were significant spatial gradients in mixing depths between the coastal and inland sites in the afternoon hours

(MacDonald et al., 2001b)

Mixing Depth Summary

- Mixing depth controls vertical dispersion of pollutants
- Same peak mixing depth can have different MGR, allowing for dissimilar pollutant concentrations
- Mixing-depth evolution is important in understanding the contribution/influence of residual-layer air on pollutant concentrations within the ABL

Transport/Flow Patterns Background

- Synoptic scale
  - Winds driven by large high- and low-pressure systems
- Meso-scale
  - Land/sea or lake breeze
  - Mountain/valley
  - Terrain-forced
- Surface vs. boundary layer
  - Transport at different levels
  - Daytime coupling

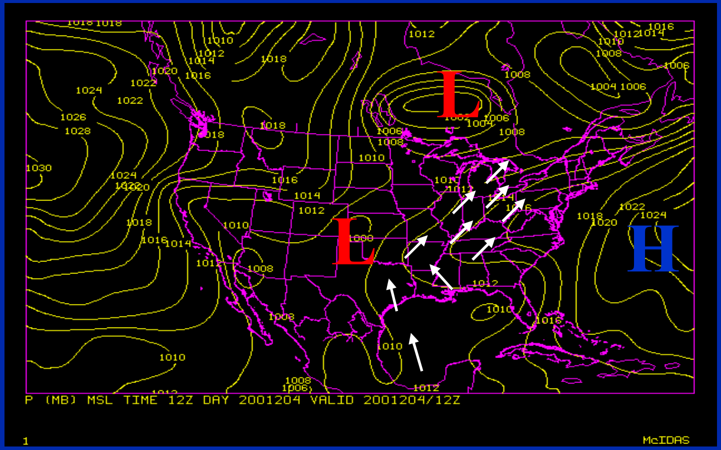

July 23, 2000 MSLP

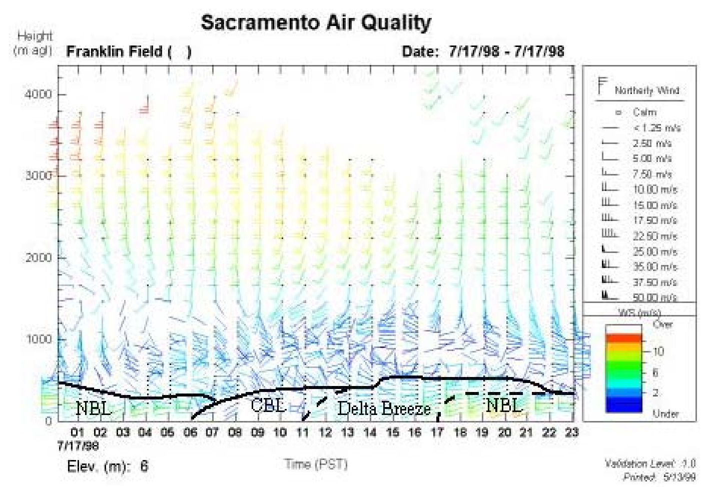

Radar profiler wind data with boundary layers at Franklin Field on July 17, 1998

Transport/Flow Patterns Data and Methods

- Data
  - RWP and Sodar provide continuous time-height cross-sections of winds
- Methods
  - Trajectories
  - Transport, ventilation, and recirculation statistics
  - Ventilation index
  - Flux planes
  - Spatial views

Transport/Flow Patterns – Data and Methods Trajectories (1 of 3)

- Large-scale NWP models (NGM, ETA, AVN, MRF, etc.) cannot resolve sub-grid scale processes
- Incorporating the RWP measurements allows for some of the sub-grid scale processes to be incorporated in the trajectory calculation
- “Trajectories” can either be forward or backward calculations and can be run at multiple heights

Transport/Flow Patterns – Data and Methods Trajectories (2 of 3)

- Use hourly wind speed and direction derived by the RWP to calculate local forward trajectories
- Work in Universal Transverse Mercator (UTM)
  - Step 1: Convert hourly wind speed (ws) and direction (wd) to U and V

    $U = -ws \times \sin(wd),\ V = -ws \times \cos(wd)$

  - Step 2: For wind at a given altitude, calculate hourly (i) parcel position (UTMx and UTMy):

    $UTMx\ (i+1) = (U \times \text{time step}) + UTMx\ (i)$

    $UTMy\ (i+1) = (V \times \text{time step}) + UTMy\ (i)$

  - Step 3: Plot UTMx and UTMy at each time

Transport/Flow Patterns – Data and Methods
Trajectories (3 of 3)

Trajectories associated with land/sea breeze circulation

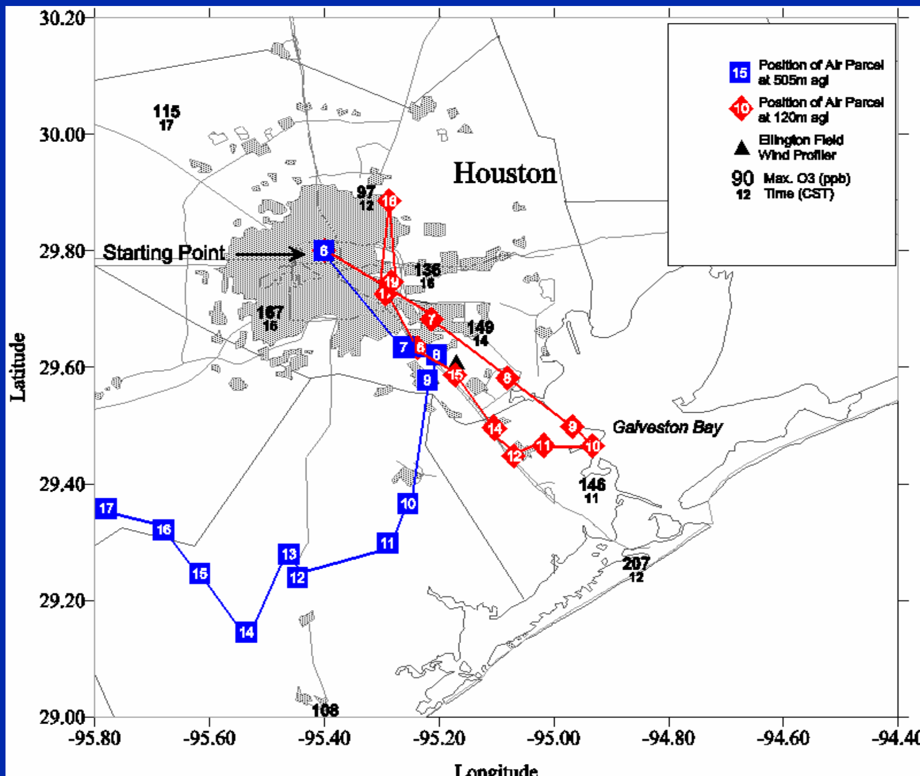

Forward 120-m agl and 505-m agl wind runs from downtown Houston (0600 to 1800 CST on August 29, 1998). Peak ozone concentrations and times of peak concentration (begin hour CST) at each monitoring site are shown (MacDonald et al, 2001c)

Weak synoptic gradient

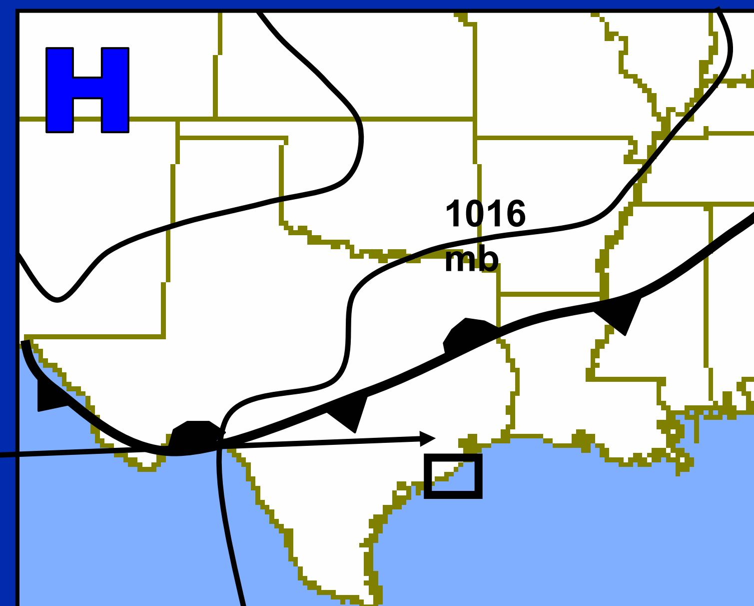

Surface pattern on August 29, 1998

Transport/Flow Patterns – Data and Methods
Transport, Ventilation, and Recirculation Statistics (1 of 4)

- Ventilation (i.e., flow-through) and recirculation analyses are used to investigate transport conditions aloft.
- The procedure discussed here is based on integral quantities computed from profiler data following the work of Allwine and Whiteman (1994).
- Parameters are typically calculated using 12 or 24 hrs of hourly wind data.
- Parameters include:

S	Scalar wind run (km)
L	Resultant (vector) transport distance (km)
Θ	Resultant wind directions in degrees from true N adjusted to the proper quadrant
R	Recirculation factor (*L/S*)

Transport/Flow Patterns – Data and Methods
Transport, Ventilation, and Recirculation Statistics (2 of 4)

Recirculation Factor

R = 1	Straight-line, steady transport occurred during integration period
R = 0	No net transport
R ≈ 1	Good ventilation conditions (for *L* = few hundred km)
R < ~0.3	Recirculation

Transport/Flow Patterns – Data and Methods

Transport, Ventilation, and Recirculation Statistics (3 of 4)

	Hour 1	Hour 2	Hour 3	Hour 4
Wind Speed (m/s)	2	2	2	2
Wind Direction	180	180	360	360

Scalar Average	2
Vector Average	0
Recirculation Factor	0

Transport/Flow Patterns – Data and Methods
Transport, Ventilation, and Recirculation Statistics (4 of 4)

- This example shows vector-integrated transport distances (top), resultant wind directions (middle), and recirculation factors (bottom) calculated from data collected by the southeast Houston RWP for the period 0600-1700 CDT on August 16, 1993.
- The transport distances in the first few hundred meters were about 175 km with the recirculation factor indicating good ventilation conditions.
- On this day, low ozone concentrations were observed, and the aloft winds showed little recirculation.

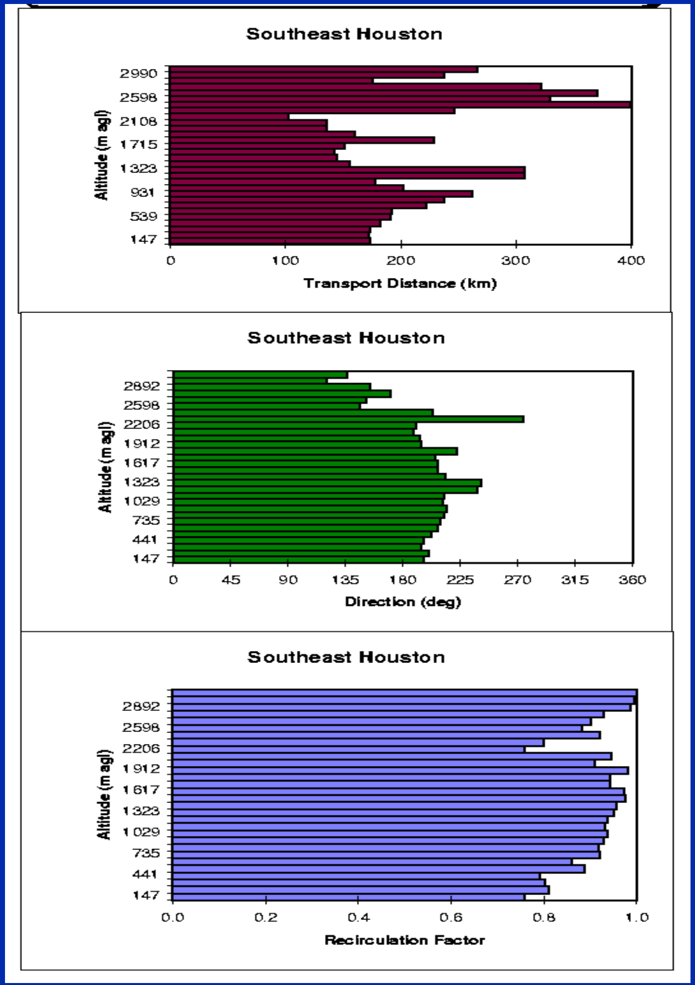

(Main & Roberts, 2000)

Transport/Flow Patterns – Data and Methods Ventilation Index

Ventilation Index = Mixing Depth x Boundary Layer Wind Speed

Good indicator of the amount the ventilation or transport of pollutants

Date	Time of Flow PDT	Wind Direction	Average Wind Speed, m/sec	Duration, hrs	Mixing Height at 0800-0900, m agl	Ventilation, m^2/sec
Aug. 4, 1997	21-07	E	2.5	11	250	625
Aug. 4, 1997	21-Aug	SW	3.3	12		
Aug. 5, 1997	22-08	E	3.5	11	275	962
Aug. 5, 1997	21-Sep	SW	2.9	13		
Aug. 6, 1997	22-07	E-NE	1.9	10	400	760
Aug. 6, 1997	21-Aug	SW	3.2	14		
Sept. 4, 1997	22-09	E	2.5	12	250	625
Sept. 4, 1997	22-Oct	SW	2.8	13		
Sept. 5, 1997	23-08	E	1.7	10	375	638
Sept. 5, 1997	20-Sep	SW	3	12		
Sept. 6, 1997	21-08	Variable	1.6	12	600	960
Sept. 6, 1997	22-Sep	SW	2.8	14		

Surface winds at Azusa, morning mixing depths at El Monte, and calculated ventilation indices (Reissell et al., 2003)

Transport/Flow Patterns – Data and Methods
Flux (1 of 3)

- Flux calculations can be used to understand the amount of pollution transported from upwind to downwind areas
- Flux, for air quality purposes, is the rate of transfer of pollutant mass per unit area per unit time ($ug/m^{-2}\ sec^{-1}$)
- Flux = Wind speed (m/sec) x Concentration (ug/m^3)
- Total amount of mass through a plane = Flux x Area x Time

Transport/Flow Patterns – Data and Methods
Flux (2 of 3)

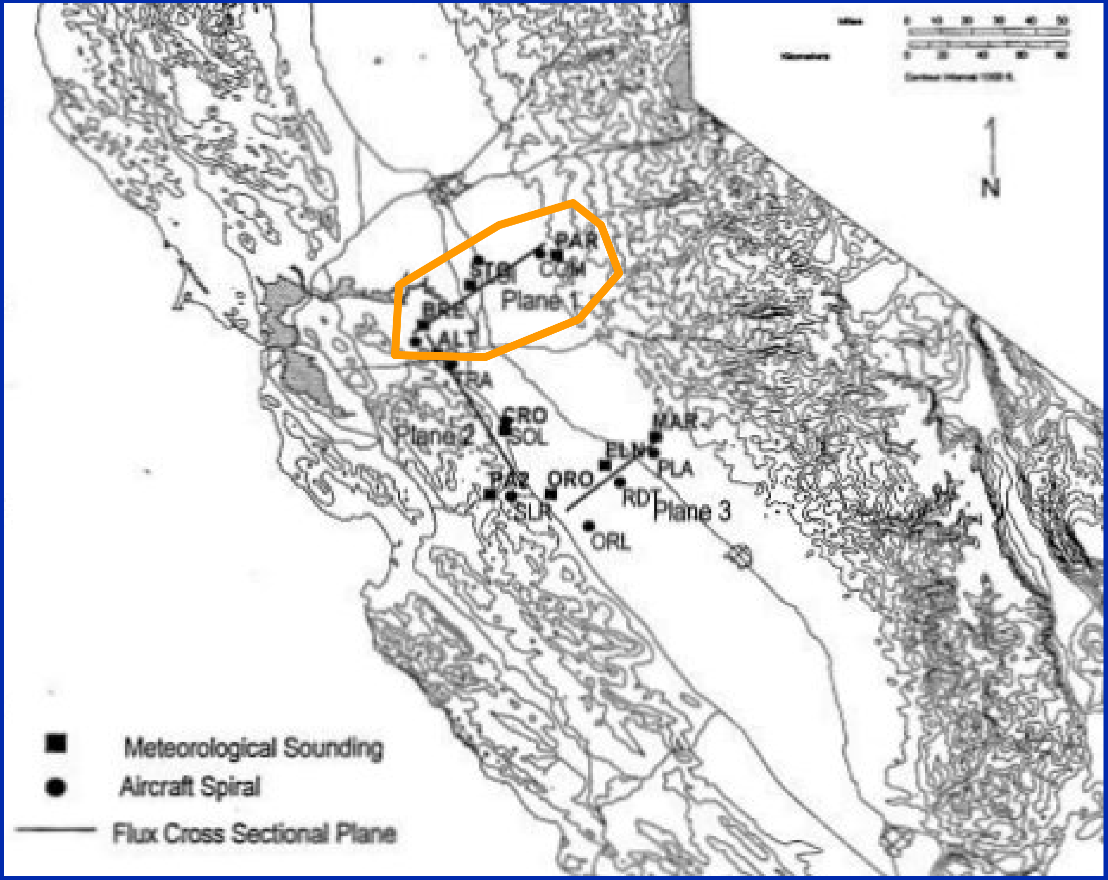

Flux cross-sectional planes across the San Joaquin Valley (Blumenthal et al., 1997)

Transport/Flow Patterns – Data and Methods Flux (3 of 3)

Finding: Amount of NO_x flowing into the San Joaquin Valley (SJV) was equivalent to NO_x emissions in the northern SJV for this day

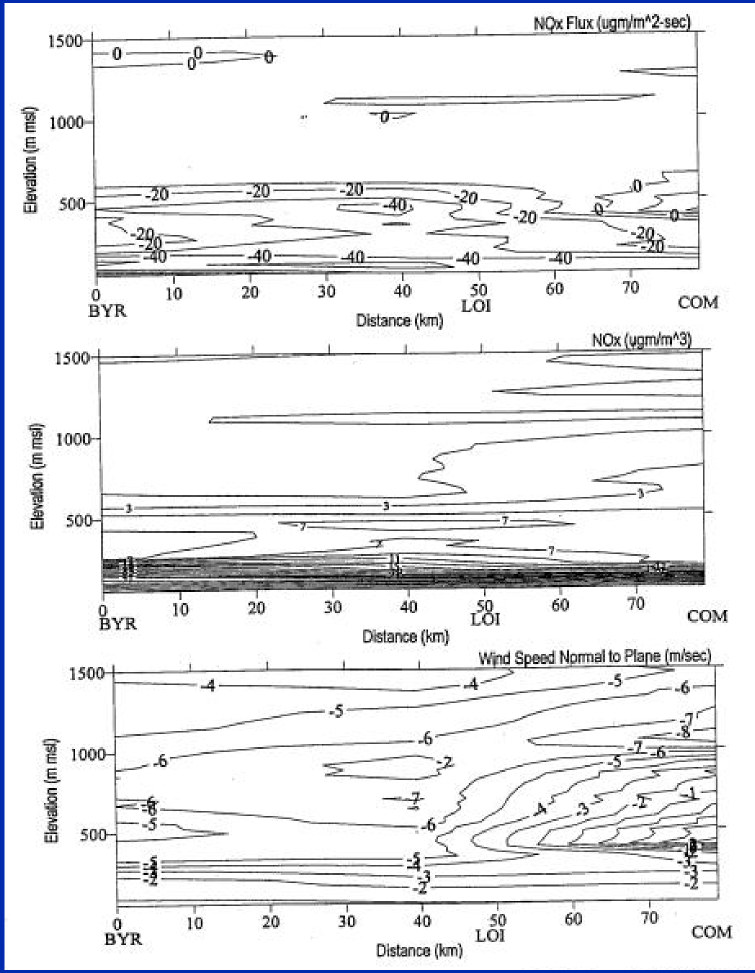

NO_x flux estimates across Plane 1 on the morning of August 6, 1990 (Blumenthal et al., 1997)

Transport/Flow Patterns – Data and Methods Spatial Views

Regional extent of low-level jet

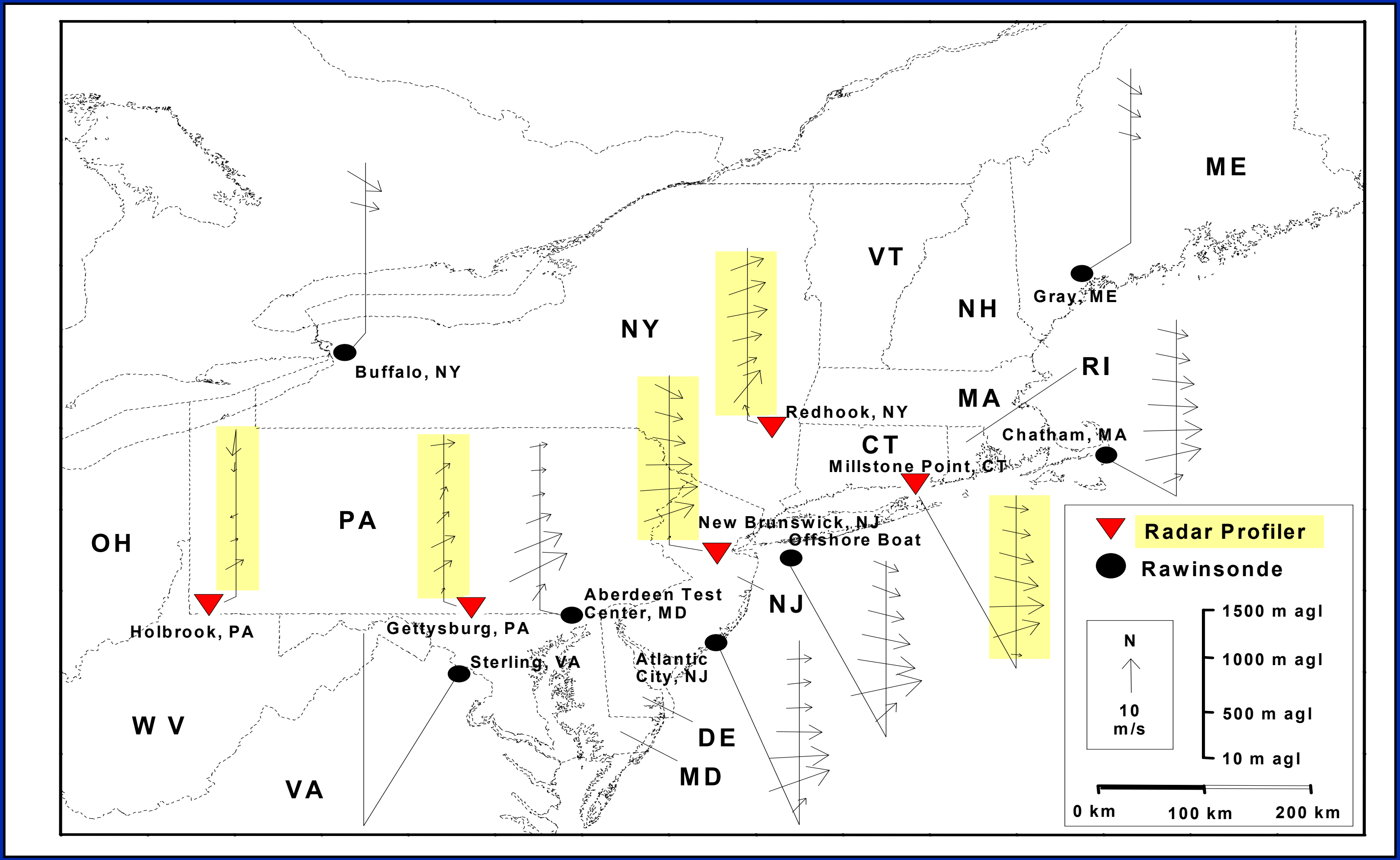

Upper-air winds on July 14, 1995, at 0300 EST, used to locate the low-level jet during an air pollution episode

Transport/Flow Patterns – Summary

- Continuous aloft wind data are useful in understanding the processes that influence local air quality
- Assessment techniques include
  - Trajectories
  - Transport, ventilation, and recirculation statistics
  - Ventilation index
  - Flux planes
  - Spatial views

Meteorological Models

- Meteorological models are used to estimate transport and dispersion parameters that affect air quality
- Meteorological and emission models provide inputs to air quality models
- Air quality models simulate physical and chemical processes in the atmosphere and are used to
  - Assess impacts from pollutant sources
  - Develop an understanding of air pollution problems
  - Design and evaluate pollution control strategies
  - Estimate the impact of emission growth and controls on future air quality

Meteorological Models – Types

- Objective Model
  - Uses profiler observations
  - Utilizes interpolation and extrapolation of observations
- Diagnostic Model
  - Uses profiler/RASS observations to provide physical relationships and parameterizations
  - Is not predictive in time (observationally limited)
  - Produces output that can be combination of objective and diagnostic analysis
- Prognostic Model
  - Predicts meteorological parameters based on time-dependent equations of atmospheric physics
  - Is predictive in time
  - Uses profiler/RASS data to
    - Set initial conditions
    - Account for sub-grid scale phenomena that is not resolved by model
    - Constrain/limit accumulation of model errors with time (model drift)
    - Quality assure model results

Meteorological Models – CALMET (1 of 3)

- The CALMET diagnostic meteorological model is a software tool that interpolates observations to a gridded field and diagnoses winds based on terrain, stability, and large-scale flow patterns
- Inputs
  - 1-km surface-terrain height
  - 1-km land-use data
  - Surface, rawinsonde, RWP, RASS, buoy, C-MAN, and EDAS data

Meteorological Models – CALMET (2 of 3)

SCOS-97 CALMET (Diagnostic Model)

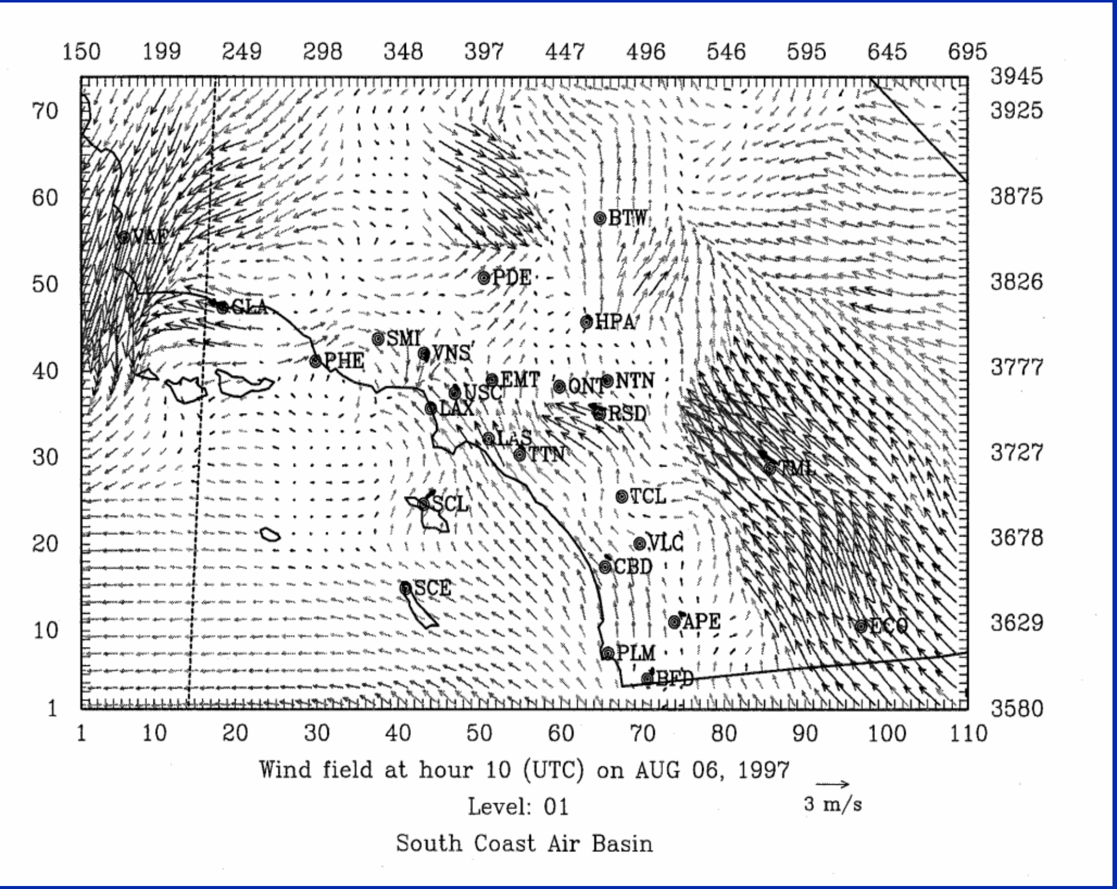

CALMET 40-m agl winds at 0300 PST on August 6, 1997 (MacDonald et al., 2000)

Meteorological Models – CALMET (3 of 3)

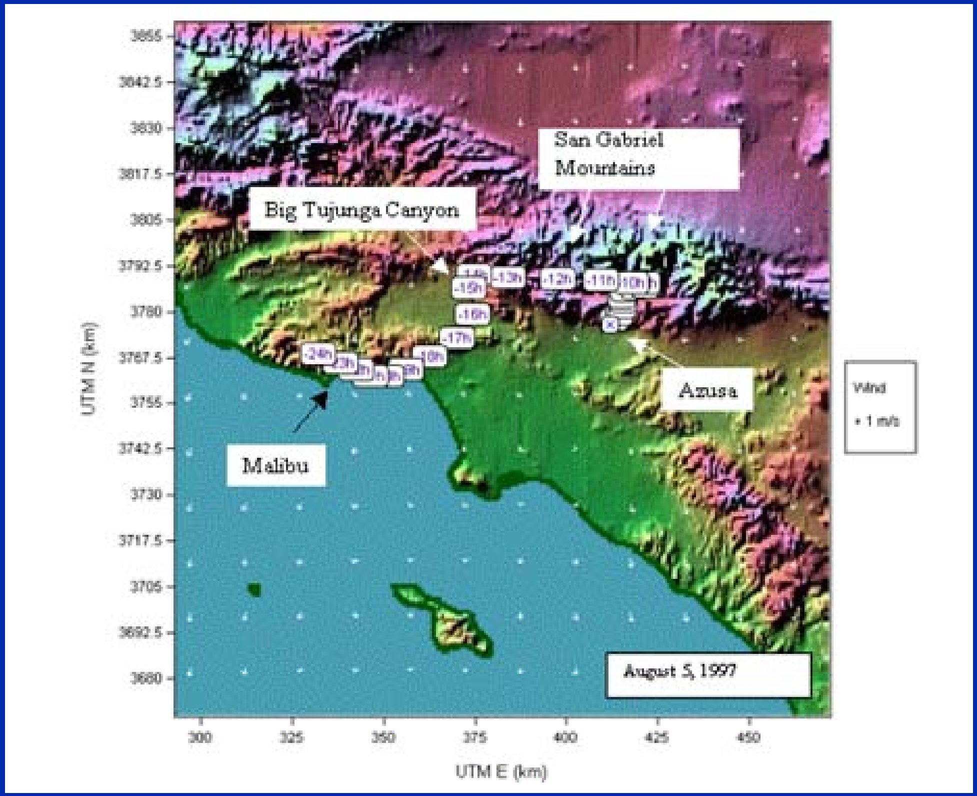

Twenty-four-hour 158-m agl back trajectory beginning at Azusa, California, at 0600 PDT on August 5, 1997. UTM E and UTM N are Universal Transverse Mercator East and North coordinates, respectively (Reissell et al., 2003).

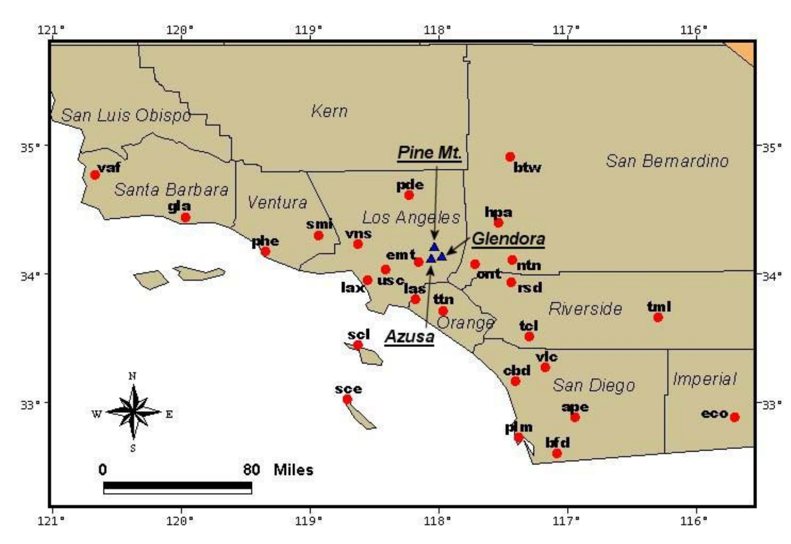

Modeling domain showing location of 26 RWP sites during the SCOS-97 field study and the locations of Azusa, Pine Mountain, and Glendora monitoring sites (Reissell et al., 2003).

Meteorological Models – Verification (1 of 2)

MM5 Output – Sacramento

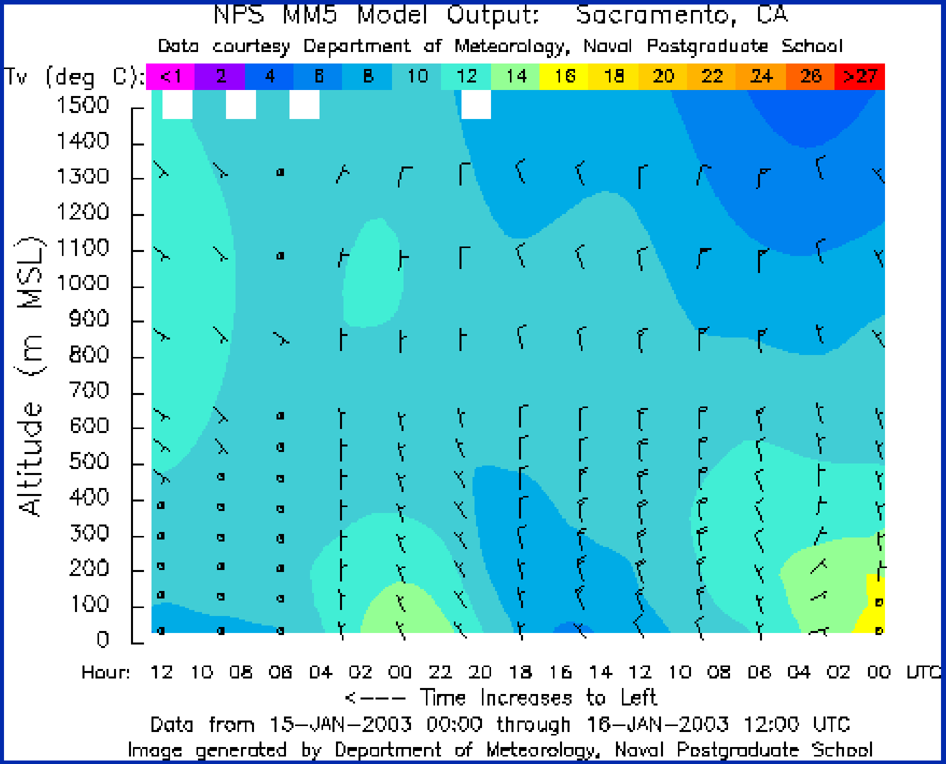

915-MHz RWP – Sacramento

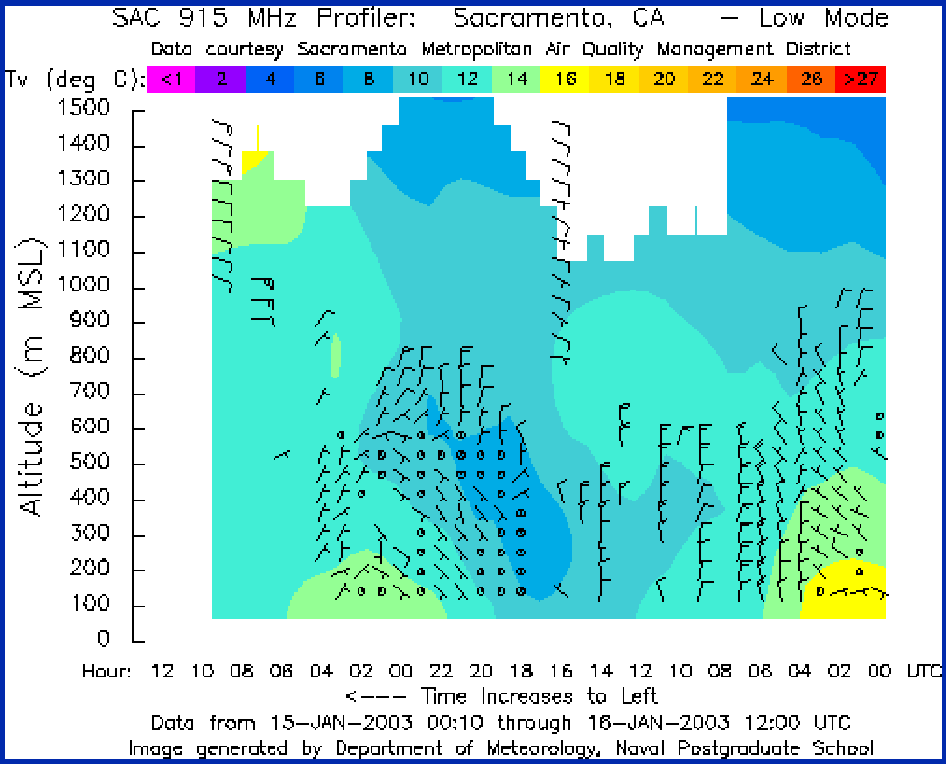

Naval Postgraduate School MM5 Real-Time Forecast
http://www.weather.nps.navy.mil/~dkmiller/MM5/

Meteorological Models – Verification (2 of 2)

SJVAQS/AUSPEX

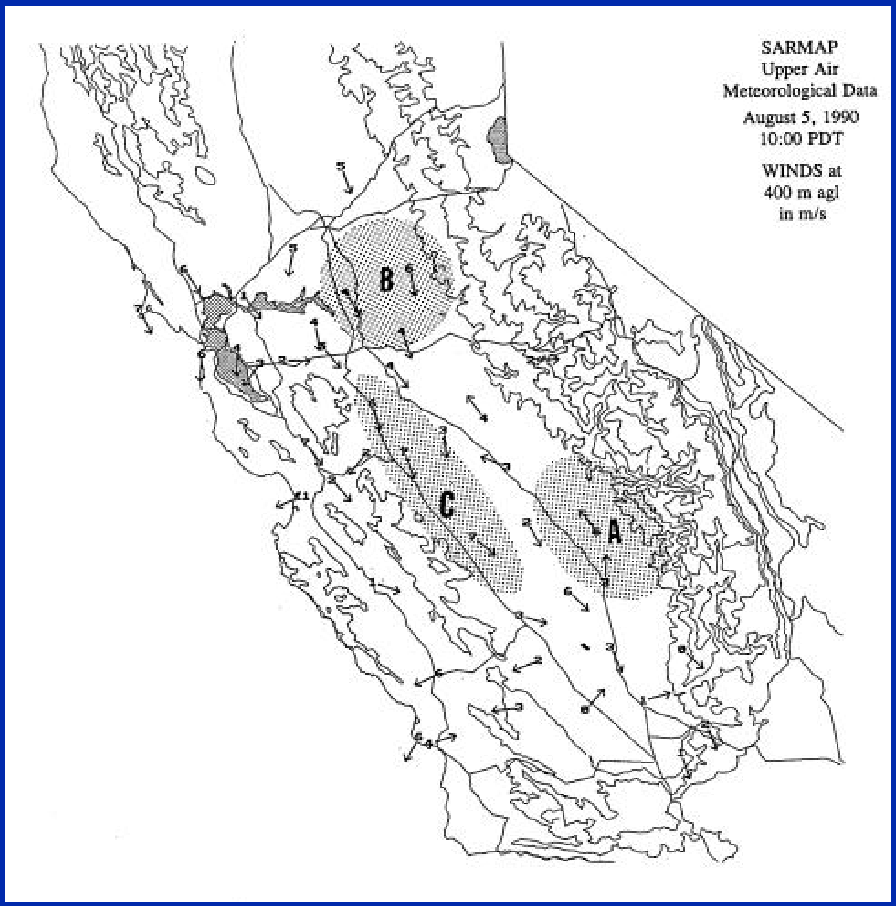

Observed 400-m agl winds on August 5, 1990, at 0900 PST

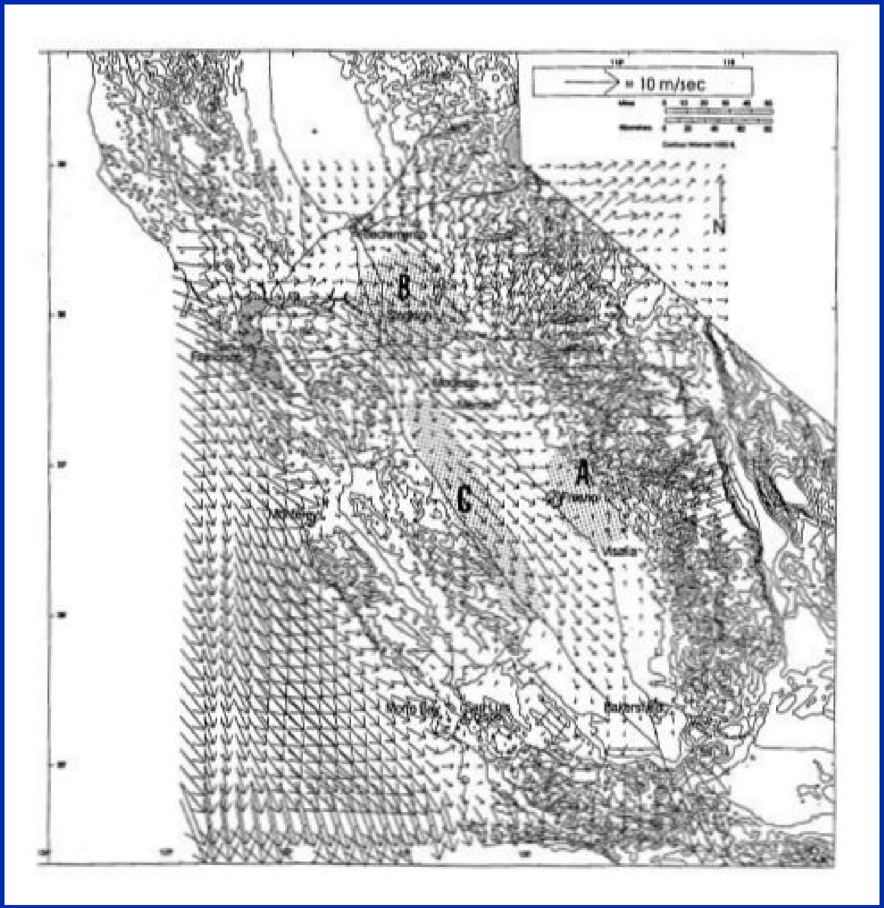

MM5 400-m agl 12-km grid model winds on August 5, 1990, at 0900 PST

(Blumenthal et al., 1997)

Meteorological Models – Summary

Continuous upper-air meteorological data are a key component of accurate diagnostic and prognostic meteorological and air quality modeling

Summary

- RWP/RASS and Sodar data are important components of solving many air quality issues
- Data supports
  - Boundary-layer characterization
  - Winds/transport assessment
  - Model inputs and evaluation

References (1 of 3)

Allwine K.J. and Whiteman C.D. (1994) Single-station integral measures of atmospheric stagnation, recirculation, and ventilation. *Atmos. Environ*. **28**, 713-721.

Angevine W.M. (1994) Boundary-layer depth and entrainment zone characterization with a boundary-layer profiler. *Boundary-Layer Meteorology.* **68**, 375-385.

Bianco L., and Wilczak J.M., (2002) Convective boundary layer depth: Improved measurement by Doppler radar wind profiler using fuzzy logic methods. *J. Atmos. Oceanic Tech.* **19**, 1745-1758.

Blumenthal D.L., Lurmann F.W., Roberts P.T., Main H.H., MacDonald C.P., Knuth W.R., and Niccum E.M. (1997) Three-dimensional distribution and transport analyses for SJVAQS/AUSPEX. Final report prepared for San Joaquin Valley Air Pollution Study Agency, Sacramento, CA, by Sonoma Technology, Inc., Santa Rosa, CA, Technical & Business Systems, Santa Rosa, CA, and California Air Resources Board, Sacramento, CA, STI-91060-1705-FR, February.

Dye T.S., Lindsey C.G., and Anderson J.A. (1995) Estimates of mixing depth from "boundary layer" radar profilers. Preprints from the *9th Symposium on Meteorological Observations and Instrumentation, Charlotte, NC, March 27-31*, pp. 156-160 (STI-94212-1451).

Lilly M.A.R. (2003) The influence of synoptic meteorology on convective boundary layer characteristics and the observed chemical response during PROPHET 2000 and 2001 summer intensives. Department of Environmental Sciences, University of Virginia, Charlottesville, VA (in progress).

References (2 of 3)

MacDonald C.P., Roberts P.T., Knoderer C.A., Miller D.S., and Hanna S.R. (2002) Boundary layer study in the western and central Gulf of Mexico. Report prepared for the Minerals Management Service, New Orleans, LA, by Sonoma Technology, Inc., Petaluma, CA, STI-998555-2266-DIR, October.

MacDonald C.P., Roberts P.T., Main H.H., Dye T.S., Coe D.L., and Yarbrough J. (2001a) The 1996 Paso del Norte Ozone Study: analysis of meteorological and air quality data that influence local ozone concentrations. *Sci. Total Environ.* (Special Issue: U.S.-Mexico Trans-boundary Air Pollution Studies) **276, Nos. 1-3**, pp. 93-110 (STI-1949).

MacDonald C.P., Dye T.S., and Roberts P.T. (2001b) Spatial and temporal observations of the planetary boundary layer during ozone episodes in Southern California. Presented at *SCOS97-NARSTO Data Analysis Conference, Los Angeles, CA, February 13-15* (STI-2057).

MacDonald C.P., Blumenthal D.L., Roberts P.T., and Crews J.M. (2001c) Analysis of 1997 through 1999 air quality data collected by the Baylor University aircraft. Report prepared for the Texas Natural Resource Conservation Commission, Austin, TX, by Sonoma Technology, Inc., Petaluma, CA, STI-900510-2033-FR, January.

MacDonald C.P., Knoderer C.A., Arndt R.L., Roberts P.T., Emery C., Stoeckenius T., and Tai E. (2000) PAMS data analysis for Southern California volume III: three-dimensional wind fields and trajectories during three SCOS97 episodes. Report prepared for South Coast Air Quality Management District, Diamond Bar, CA, by Sonoma Technology, Inc., Petaluma, CA, STI-997526-1960-DFR, March.

References (3 of 3)

MacDonald C.P., Chinkin L.R., Dye T.S., and Anderson C.B. (1999) Analysis of PAMS data in California Volume I: The use of PAMS radar profiler and RASS data to understand the meteorological processes that influence air quality in selected regions of California. Report prepared for the U.S. Environmental Protection Agency, Research Triangle Park, NC, by Sonoma Technology, Inc., Petaluma, CA, STI-998391-1888-FR, May.

Main H.H. and Roberts P.T. (2000) PAMS Data Analysis Workbook: Illustrating the use of PAMS data to support ozone control programs. Prepared for the U.S. Environmental Protection Agency, Research Triangle Park, NC, by Sonoma Technology, Inc., Petaluma, CA, STI-900243-1987-FWB, September.

Reissell A., MacDonald C., Roberts P., and Arey J. (2002) Characterization of BVOC'S and meterology at Azusa during the 1997 Southern California Ozone Study. Atmos. Environ. (submitted for publication).

Watson J.G., Fujita E.M., Chow J.C., Zielinska B., Richards L.W., Neff W., and Dietrich D. (1998) Northern front range air quality study. Final report prepared for Colorado State University, Cooperative Institute for Research in the Atmosphere, Fort Collins, CO by Desert Research Institute, Reno, NV, June.